Chemistry
Europe
European Chemical
Societies Publishing

Recent Advances in Synthesis of Molecular Heteroleptic Osmium and Iridium Phosphorescent Emitters

María L. Buil,[a] Miguel A. Esteruelas,*[a] and Ana M. López[a]

The application of new procedures of organometallic synthesis based on alternative starting complexes has given rise to a significant enhancement in the preparation of osmium(IV), osmium(II), and iridium(III) emitters, since 2012. The choice of the precursors should be done taking into account its ligands, since they may cooperate in the emitter synthesis. Three different functions are clearly pointed out in the revised procedures: the ligands of the starting compounds can direct the selectivity of competitive ruptures of σ-bonds of the chromophores, without having direct participation in the activation; on the contrary, they can directly participate in the generation of a ligand, being a part of the new coordinated group; and the ligands can also act as internal base in σ-bond heterolytic activation reactions. In addition, the ability of the polyhydrides $OsH_6(P^iPr_3)_2$ and $IrH_5(P^iPr_3)_2$ to activate C—H bonds is pointed out as one of the determining factors of the success in many cases.

1. Introduction

Organic-light-emitting-diode (OLED) technology is viewed as the immediate future for display and lighting applications, particularly OLEDs employing phosphorescent emitters (PHO-LEDs). The relevance of PHOLEDs is due to their better characteristics compared to devices using fluorescent emissive compounds.[1] Phosphorescent emitters based on 5d metals display a fast intersystem crossing between the lowest-lying singlet and the emissive triplet excited states,[2] which enable them to harvest both singlet and triplet excitons and to reach internal quantum efficiency almost 100%.[3] Green and red PHOLEDs have achieved the commercial requirements for the lighting and display fields. On the contrary, blue PHOLEDs remain a challenge. While cationic transition-metal complexes are mainly employed for light-emitting electrochemical cells,[4] neutral-charge compounds are the preferred ones for the fabrication of PHOLEDs by vacuum thermal evaporation.[5] This latter deposition method is the predominant one in commercial manufacturing.

The highest occupied molecular orbital (HOMO) of the emitters involves the metal and some of its ligands, whereas the lowest unoccupied molecular orbital (LUMO) extends on π^* orbitals of some ligand. As a consequence, the HOMO–LUMO gap and the energy of the excited states are metal and ligand dependent and therefore can be controlled by a judicious selection of the metal and ligands of the emissive complex. For instance, osmium(II) affords shallower HOMO energy levels than iridium(III). Thus, most of the luminescent osmium(II) compounds emit from green to red, being easier to get blue emission from iridium(III) complexes.[2a,6] The presence of electron-withdrawing groups in the phenyl moiety of an orthometalated 2-phenylpyridine usually produces a blue shift with respect to the unsubstituted chromophore,[7] while the increase of the conjugation of the heterocycle by fused aromatic rings gives rise to a red shift.[8] Hence, in principle, it is conceivable to design stable complexes with tailored photophysical properties in agreement with the requirements of a given application.

There is certainly great interest in phosphorescent emitters of osmium and iridium. Out of the two, those of osmium are the least developed, essentially because of the difficulty of their synthesis.[6,9] By contrast, the iridium(III) emitters are situated at the vanguard of the current photophysics[5,10] and photochemistry.[11] With some exceptions,[12] the majority of the emissive compounds of these elements are homoleptic or heteroleptic mononuclear derivatives. Homoleptic compounds are molecules formed by a metal core surrounded by equal ligands. Heteroleptic complexes bear at least two different ligands. Taking into account the denticity and the number of electrons donated, the ligands can be grouped into: monodentate donating 1 or 2 electrons (1m and 2m); bidentate donating 2, 3, or 4 electrons (2b, 3b, and 4b); tridentate donating 3, 4, 5, or 6 electrons (3t, 4t, 5t, and 6t); and tetradentate donating 6 or 7 electrons (6tt and 7tt).

Heteroleptic compositions allow a better fine tuning of the photophysic features of the emitters than the homoleptic ones.[10c,e,13] As a consequence, OLED research companies display a great interest in heteroleptic emitters. In this context, it should be noted that for a given heteroleptic composition, a number of isomers with different stereochemistry are feasible, with increasing number of isomers as the number of different donor atoms around the metal center increases. Furthermore,

[a] Dr. M. L. Buil, Prof. Dr. M. A. Esteruelas, Prof. Dr. A. M. López
Departamento de Química Inorgánica
Instituto de Síntesis Química y Catálisis Homogénea (ISQCH)
Centro de Innovación en Química Avanzada (ORFEO-CINQA)
Universidad de Zaragoza-CSIC, 50009 Zaragoza, Spain
E-mail: maester@unizar.es
https://esteruelasgroup.com

EurJIC
European Journal of Inorganic Chemistry

Minireviews
doi.org/10.1002/ejic.202100663

Chemistry Europe
European Chemical Societies Publishing

each isomer can have its own photophysical characteristics. Thus, selective synthesis of the preferred isomer is highly desirable. An additional issue, to the existence of structural isomers, is the high tendency of the heteroleptic complexes to produce mixtures of compounds as a result of ligand redistribution equilibria. The preparation methods involving one-pot procedures give statistical blends of ligand distribution products, where the maximum yield of each one is already low before the necessary column chromatography separation.[14] The synthesis through the consecutive coordination of the ligands is a tedious multi-step procedure,[15] which has only a partial success when they are very different. Three approaches have been principally used to solve these challenges: selective ligand post-functionalization,[16] decrease of groups around the metal center by using ligands with higher denticity,[13b,17] and binding different ligands by means of a linker.[18] The former usually requires the use of catalysts, whereas the second and third approaches give rise to more rigid systems. At first, distortions associated to the rigidity were considered a disadvantage for the emission efficiency.[19] However, it was soon realized that increasing the strength of the metal-ligand bond may on the contrary have positive effects, in addition to increase the stability of the emitter.[20] By this way, tetradentate ligands have been employed as tools to enhance the photoluminescence quantum yield (Φ) of d^8 ion complexes,[21] even of those with weaker spin–orbit coupling and thermally accessible metal-centered d–d states.[22]

The development of efficient synthetic methodologies to the preparation of heteroleptic phosphorescent emitters with bespoke photophysical properties is currently one of the biggest demands of the OLED companies. Our research group is not unfamiliar with this need and is strongly working on it since 2012. This account contextualizes our effort on the design and development of new synthetic procedures to the synthesis of emitters of this class based on osmium and iridium.

2. Osmium(IV) Emitters

Osmium(II) complexes show not easy color tuning, particularly with respect to the high energy region, as a consequence of the small HOMO–LUMO gap. Osmium(IV) species with a pentagonal-bipyramidal structure exhibit a deeper HOMO level, which in principle makes easier to reach the high energy region. Thus, osmium(IV) compounds, in addition to being more difficult to oxidize than osmium(II) ones, can offer more flexibility for color tuning. Moreover, OLED devices based on osmium(IV) emitters should be more resistant to the formation of an exciplex.[23] Although PHOLEDs based on osmium(IV)-emitters are undoubtedly promising and challenging, emissive complexes of this central ion have received limited attention. This may be due in part to the difficulty of their synthesis and the believe that the facile interconversion between the several structures possible for these compounds, which are close in energy, could lead to a dynamic quenching of the phosphorescence.

Polyhydrides of platinum group metals have proven an amazing ability to activate σ-bonds. In agreement with it, the d^2-hexahydride $OsH_6(P^iPr_3)_2$ (**1**) enables the activation of C–H bonds of a wide variety of organic molecules,[24] including some chromophore. Such ability has opened the door to emissive osmium(IV) compounds. This first generation includes dihydride and trihydride derivatives of the general formulas $OsH_3(XY)(P^iPr_3)_2$ and $OsH_2(XYZ)(P^iPr_3)_2$, which bear chelate and pincer chromophores, respectively.

Complex **1** activates the $C(sp^2)$–H bond at 3-position of the [*4*]-carbohelicene substituent of 1-methyl-4-(2-pyridyl)benzo[*g*] phenantrene and its 2-pyrazinyl counterpart. The reactions lead

Miguel A. Esteruelas was born in Zaragoza and attended University of Zaragoza. After obtaining his Ph.D. in December 1983, he worked as a postdoctoral fellow in the laboratory of Prof. Helmut Werner at the University of Würzburg. In 1985, he returned to the University of Zaragoza to be promoted to Professor of Inorganic Chemistry in 1988 and to Distinguished Professor in 2003. In 2007, he moved to the Spanish Research Council (CSIC), where he is currently Research Professor at the Instituto de Síntesis Química y Catálisis Homogénea (ISQCH). Esteruelas' research group focuses its interest in organometallics. Emphasis is placed on the use of transition metal hydride complexes for the activation of σ-bonds and the generation of metal–carbon multiple bonds, and the implication of such reactions in catalysis and material synthesis.

María L. Buil studied Chemistry at the University of Zaragoza (Spain) and obtained her Ph.D. in 1997 under the supervision of Prof. Miguel A. Esteruelas. After a two-year postdoctoral stay in the group of Robin N. Perutz at the University of York (U.K.), she returned to the University of Zaragoza where she is currently Associate Professor of Inorganic Chemistry. Her research interest focuses on the chemistry of organometallic complexes and their catalytic applications and the synthesis of phosphorescent emitters.
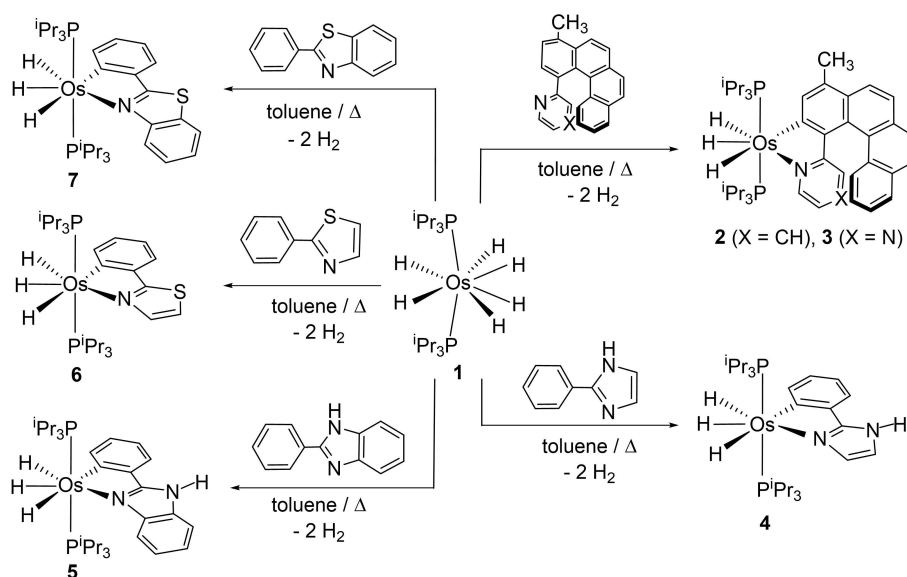
Ana M. López studied Chemistry at the University of Zaragoza (Spain) where she obtained her Ph.D. in 1991 under the supervision of Profs. M. Pilar García and Luis A. Oro. Then she joined to the group of Prof. Esteruelas. Since 2012, she is full Professor at the Inorganic Chemistry Department of the Zaragoza University. Her current research interest concerns organometallic chemistry of the platinum group metals and their applications in homogeneous catalysis and synthesis of phosphorescent emitters.
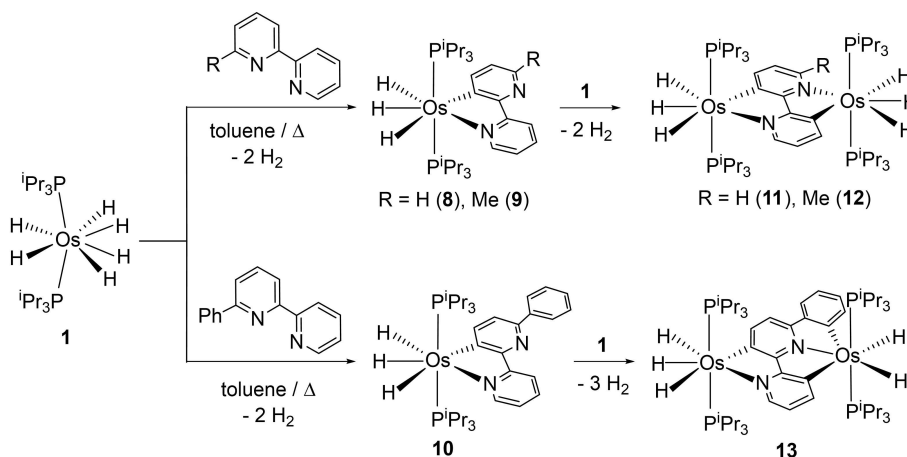
EurJIC
European Journal of Inorganic Chemistry

Minireviews
doi.org/10.1002/ejic.202100663

Chemistry
Europe
European Chemical
Societies Publishing

to the [6]-azaosmahelicene derivatives **2** and **3** (Scheme 1). These trihydride-d⁴-heterometalahelicenes are red phosphorescent emitters (624–683 nm) both in solid state, at 298 and 77 K, and in different solvents such as methanol, acetone, tetrahydrofuran, dichloromethane, and toluene, at 77 K.[25] Similarly to the [4]-carbohelicene substituent, the phenyl group of 2-phenyl-imidazole, -benzimidazole, -thiazole, and -benzothiazole undergoes *ortho*-CH bond activation to give the corresponding trihydride-osmium(IV) complexes **4–7**, which are also emissive when photoexcited, in the solid state and in toluene solution, at 298 and 77 K. As expected, the emission energy decreases when the NH group is replaced by a sulfur atom and with the existence of a fused six-membered ring in the azole. Thus, imidazole derived complexes **4** and **5** exhibit blue and green emission (490–515 and 564–581 nm), respectively, whereas the thiazol compound **6** emits in the yellow region (588–607 nm)

and complex **7**, bearing a benzothiazole group, is red emissive (654–683 nm).[26]

Hexahydride complex **1** also causes the rollover cyclometalation of 2,2'-bipyridines to give the corresponding cyclometalated products, including the trihydride derivatives **8–10** as a result of the C—H bond activation of 2,2-bipyridine, 6-metyl-2,2'-bipyridine, and 6-phenyl-2,2'-bipyridine (Scheme 2). The activation of the more sterically accessible positions is kinetically preferred. However, the isolated products result from a thermodynamic control of the reactions. Thus, the selectivity observed is the result of the trapping, by the heteroatom of a pyridyl ring, of the intermediate resultant from the activation of an *ortho*-CH bond of the other pyridyl unit, despite this position is sterically encumbered and therefore its activation is slow.[27] The orthometalated bipyridine ligands of complexes **8–10** undergo further cyclometalation promoted by a second molecule of **1**. Complexes **8** and **9** afford the binuclear-hexahydrides

Scheme 1. Preparation of complexes **1**–**7**.

Scheme 2. Preparation of complexes **8**–**13**.

EurJIC
European Journal of Inorganic Chemistry

Minireviews
doi.org/10.1002/ejic.202100663

Chemistry
Europe
European Chemical
Societies Publishing

11 and **12**. They result from the *ortho*-CH bond activation of the N-coordinated ring and the coordination of the nitrogen atom of the cyclometalated pyridyl ring. The hexahydride **1** is also able of activating the phenyl substituent of complex **10**, which undergoes an additional orthometalation to afford the pentahydride **13**. In contrast to **11** and **12**, complex **13** is formed by two different osmium(IV) fragments bridged by an asymmetric pentadentate ligand, which acts as a monoanionic *C,N*-chelate with the trihydride $OsH_3(P^iPr_3)_2$ unit and as a dianionic *C,N,C*-pincer with the dihydride $OsH_2(P^iPr_3)_2$ moiety.[28]

The HOMO of the binuclear derivatives **11**–**13** spreads out over the osmium-bridge-osmium system (Figure 1) with comparable participation of the three fragments, whereas the LUMO is mainly centered on the bridging heterocycle. The cyclic voltammograms of **11**–**13** exhibit three quasi-reversible oxidation peaks ($[Os_2]/[Os_2]^+$, $[Os_2]^+/[Os_2]^{2+}$, and $[Os_2]^{2+}/[Os_2]^{3+}$). The separations between successive waves are long, which yields large values of the comproportionation equilibrium constant K_c (eq 1, $n = 4$, 5), suggesting the formation of class III radicals, in agreement with the Robin-Day classification, with the odd electron fully delocalized.[29] UV-vis-NIR spectroelectrochemical studies on **12** and **13**, revealed intervalence charge transfer transition (IVCT) bands in the spectra of the monocations, which are the key characteristic of a mixed-valence species. Upon oxidation of $[12]^+$ to $[12]^{2+}$ the IVCT band disappears. However, an intense IVCT was observed in the spectrum of $[13]^{2+}$. On the basis of this spectrum and DFT calculations, cation $[13]^{2+}$ was described as a diradical. The spectrum of both trications also showed IVCT bands. According to the values of the delocatization parameter,[30] cation $[12]^{3+}$ fits into class II, whereas ITCV bands of the cations resultant from the three consecutive oxidations of complex **13** give values, which belong to class III. Cation $[12]^+$ seems to be a species of the borderline class II/class III.

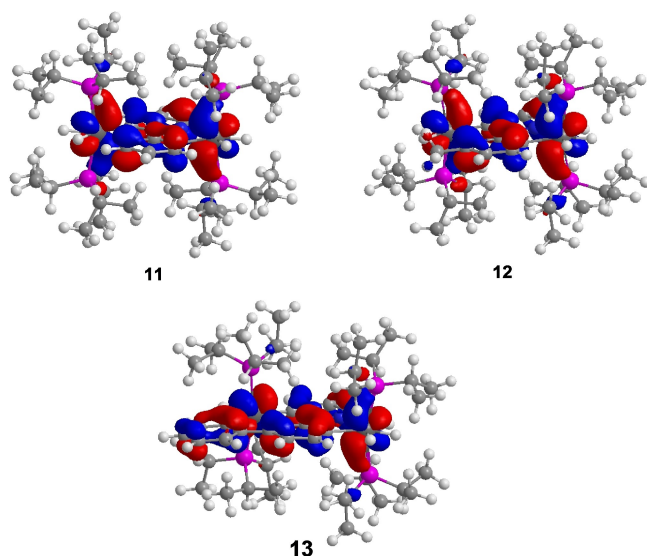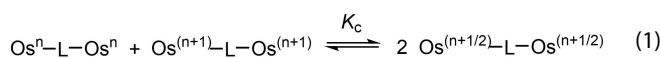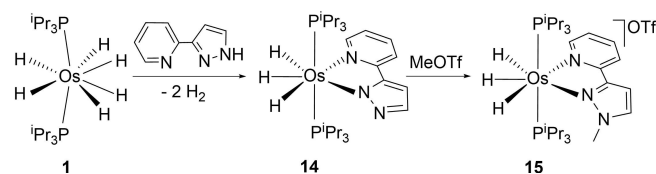The mononuclear complexes **8**–**10** and binuclear derivatives **11**–**13** are orange-red phosphorescent emitters (546–728 nm) upon photoexcitation, in doped poly(methyl methacrylate) (PMMA) film at 5 wt% at 298 K and 2-methyltetrahydrofuran (2-MeTHF) at 298 K and 77 K. Their emission spectra are very similar, which is in agreement with the small differences found between the compounds, for the DFT calculated HOMO–LUMO energy gaps (3.26–3.54 eV). The observed lifetimes are between 1.5 and 5.2 μs. The quantum yields are low (1–8%) being higher for the binuclear compounds than for the mononuclear species. This poor efficiency has been ascribed to the low values of the radiative rate constants.[28]

Complex **1** also activates the N–H bond of 2-(1*H*-pyrazol-3-yl)pyridine. The activation leads to **14**, bearing the *N,N'*-pyrazolate-pyridyl chromophore. The reaction of **14** with methyl trifluoromethanesulfonate (MeOTf) produces the methylation of the free nitrogen atom of the pyrazolate group to give the salt **15** (Scheme 3). Complex **14** and salt **15** are also emissive in the orange-red (553–660 nm) region with quantum yields, in PMMA film at 5 wt%, of 0.20 and 0.08, respectively.[31]

$$Os^n\text{–}L\text{–}Os^n + Os^{(n+1)}\text{–}L\text{–}Os^{(n+1)} \underset{}{\overset{K_c}{\rightleftharpoons}} 2\ Os^{(n+1/2)}\text{–}L\text{–}Os^{(n+1/2)} \quad (1)$$
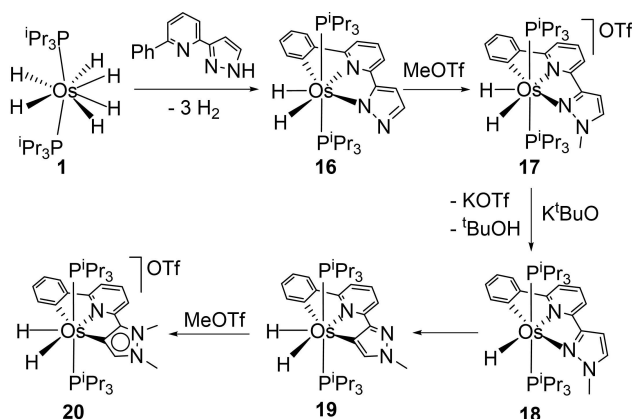
The dihydride-osmium(IV) emitters reported so far generally display modest quantum yields and, in some cases, low stability. To improve the efficiency as well as the stability of this class of emitters, the chelating chromophore was replaced by a pincer. It was thought that the higher strength of the metal–ligand bonding, because of the triple interaction, should exert a positive effect on the thermal induced extinction.[20] The chromophores used for this aim include *N,N',C*–, *C,N,C'*–, *C,N,C*–, and *N,C,C'*-donor dianions.

Complex **1** activates a bond of each substituent of 2-phenyl-6-(1*H*-pyrazol-3-yl)pyridine, namely, an *ortho*-CH of the phenyl and the N–H of the pyrazolyl. The cleavages afford the osmium(IV) dihydride derivative **16**, which coordinates a dianionic *N,N'C*-pincer ligand (Scheme 4) to form a planar metallapolycycle containing five fused rings. The dianionic ligand of **16** can be transformed into a monoanionic counterpart through the reaction with MeOTf, which adds the methyl group to the free nitrogen atom of the pyrazolyl moiety, to give the salt **17**. Its dihydride cation has Brønsted–Lowry acid character. The reaction with K^tBuO gives the osmium(II) monohydride **18**, as a consequence of the deprotonation and simultaneous reduction of the metal center. The pincer coordination of the tridentate ligand enforces a *trans*-C–Os–N angle of around 150°, quite different from the ideal value of 180° for an octahedron. This destabilizes the 2+ oxidation state of the metal ion, while it favors the 4+ oxidation state with a pentagonal-bipyramidal structure. As a result, the monohydride

Figure 1. HOMO of complexes **11**–**13**.

Scheme 3. Preparation of complexes **14** and **15**.

EurJIC
European Journal of Inorganic Chemistry

Minireviews
doi.org/10.1002/ejic.202100663

Chemistry Europe
European Chemical
Societies Publishing

Scheme 4. Preparation of complexes 16–20.

Figure 2. Emission spectra of complexes 14–17 and 19 in 2-MeTHF at 298 K.

osmium(II) complex **18** is unstable in toluene solutions, at room temperature, evolving into the dihydride osmium(IV) derivative **19** by dissociation of the pyrazolyl group and succeeding oxidative addition of the C–H bond at 4-position of the pyrazolate ring. The transformation causes a change in the pincer ligand from monoanionic *N,N′,C* to dianionic *C,N,C′*. The new *C,N,C′* ligand imposes the same structural rigidity as the *N,N′,C* pincer. Similarly to **16**, compound **19** transforms its dianionic *C,N,C′*-pincer ligand into monoanionic, by reaction with MeOTf. The addition of the methyl group to the free nitrogen atom, which yields **20**, converts the pyrazolyl moiety into a remote N-heterocyclic carbene.[31]

The *N,N′*-moiety of the pincer of the dihydride complexes **16** and **17** is similar to the chelating *N,N′*-chromophore of the trihydride compounds **14** and **15**. In agreement with this, dihydrides **16** and **17**, as well as **19**, are also orange-red emissive (590–685 nm). The comparison of the photophysical features of both classes of emitters revealed some interesting findings. While the denticity of the polydentate ligand has little effect on the emission color and the lifetimes, which are between 0.8 and 5.8 μs, it does determine the quantum yield in PMMA film (5 wt%). The molecular dihydrides **16** and **19**, possessing a pincer ligand, reach quantum yields of 0.59 and 0.45, which are threefold and twofold, respectively, the quantum yield of **14**, bearing the chelating chromophore, whereas the quantum yield of the pincer salt **17** (0.16) is twice that of the salt **15**. A noticeable feature, which is evident in the spectra in 2-MeTHF at 298 K (Figure 2), is that the rigidity enforced by the pincer ligands result in narrower emissions. This characteristic, which is highly desirable for the OLED application, seems to be due to a less marked difference between the structures of the excited-state and the ground-state.[13b,32]

The transformation of **18** into **19** is a clear proof supporting the use of the pincer bite angles as a tool for stabilizing particular oxidation states of the central ion of the emitter. The bite angles of a pincer can be judiciously modified through the introduction of adequate variations in the ligand, away fro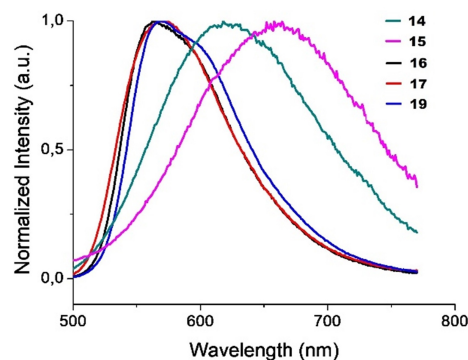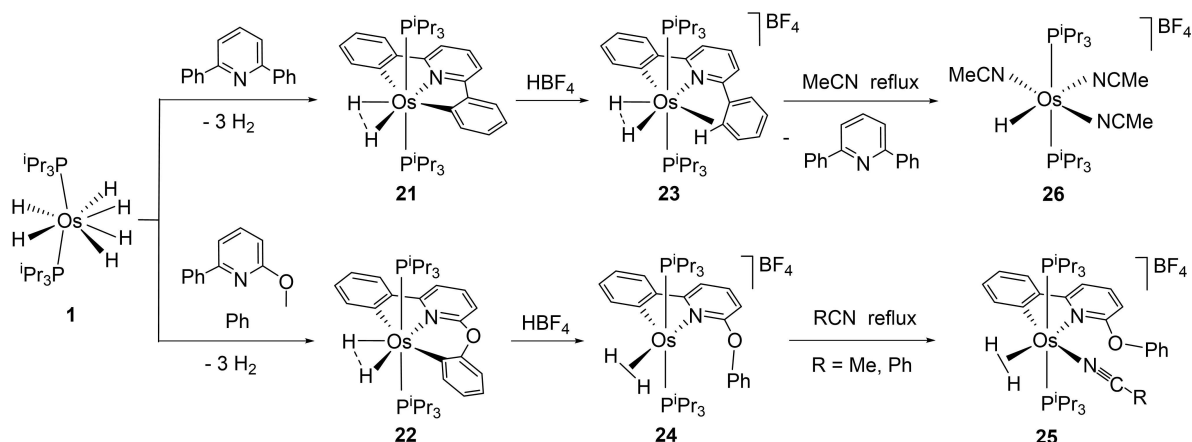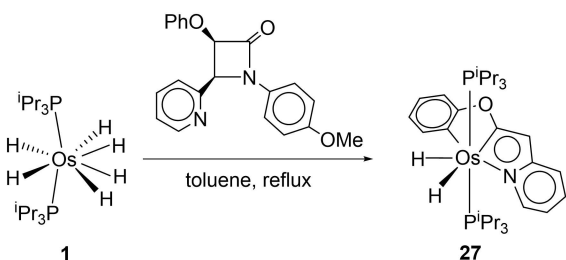m the donor atoms. For instance, the attachment of an oxygen atom between the pyridine and one of the phenyl substituents of 2,6-diphenylpyridine affords 2-phenoxy-6-phenylpyridine. The latter should give rise to a *trans*-C–M–C bite angle more open than the former. To better understand the effect of this angle on the photophysical properties of the OsH$_2$(XYZ)(P^{i}Pr$_3$)$_2$ emitters, the reactions of **1** with both pyridines was also investigated (Scheme 5).[33] Treatment of the hexahydride with the pyridines, in toluene, under reflux yields the compressed dihydrides **21** and **22**, bearing the corresponding *C,N,C*- and *C,N,C′*-pincer ligands. Although both pyridines react of the same manner, the difference between them has a remarkable chemical influence. 2,6-Diphenylpyridine promotes the formation of the osmium(IV) compound **23**, as a result of the addition of HBF$_4$ to **21**, whereas 2-phenoxy-6-phenylpyridine favors the stabilization of the osmium(II) elongated dihydrogen species **24** and **25**, in the reaction of **22** with HBF$_4$ and then with acetonitrile. Complex **23** also has a higher propensity to experience the reductive elimination of the orthometalated phenylpyridine than **24**. In acetonitrile, the reductive elimination gives **26**. Osmium(IV) compounds **21** and **22** display yellow emission. However, while complex **21** exhibits a quantum yield of 0.56 in 2-MeTHF at 298 K, its counterpart **22** is poorly emissive, showing a quantum yield of 0.03 under the same conditions. The presence of an oxygen atom between the pyridine ring and one of its phenyl substituents, which opens the C–Os–C′ angle, disfavors the 4+ oxidation state of the osmium and ruins the efficiency of the emitter.[34]

Hexahydride **1** is perhaps the transition metal-polyhydride with the maximum ability to activate σ-bonds. Accordingly, it has been used to carry out infrequent bond ruptures, including the B-type fragmentation of the four-membered ring of β-lactams. The reaction with (±)-*cis*-1-(4-methoxyphenyl)-3-phenoxy-4-(pyridine-2-yl)azetidin-2-one affords the compressed dihydride **27**, bearing a dianionic *C,C′,N*-pincer ligand, as a result of the degradation of the azetidone core and the additional *ortho*-CH bond activation of the phenoxy substituent (Scheme 6). Complex **27** is yellow emissive (540–571 nm) on photoexcitation in solid state at 298 K and in toluene solution at 298 and 77 K. The lifetimes are between 1.1 and 6.6 μs, whereas the emission quantum yield is 0.06 in the solid state.[35]

EurJIC
European Journal of Inorganic Chemistry

Minireviews
doi.org/10.1002/ejic.202100663

**Chemistry
Europe**
European Chemical
Societies Publishing

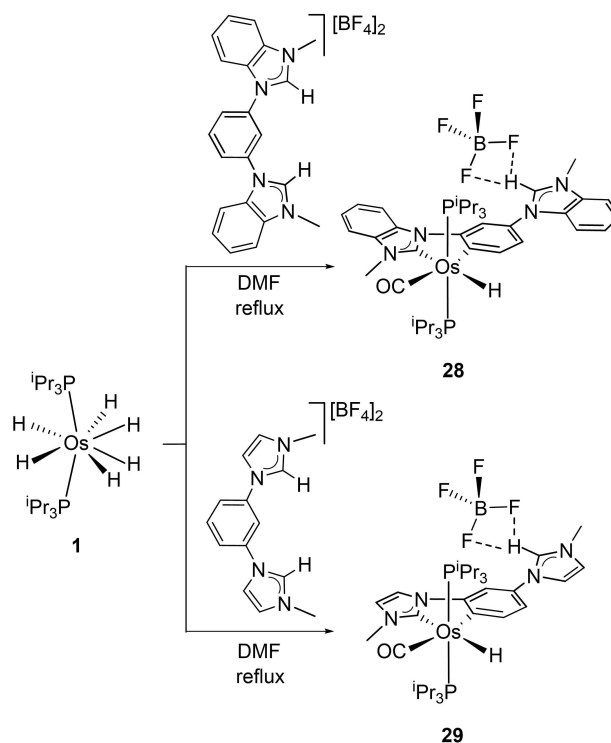**Scheme 5.** Preparation of complexes **21**–**25**.

Scheme 6. Preparation of complex **27**.

3. Osmium(II) Emitters

Molecular emitters of this class have been traditionally based on carbonyl, orthometalated aryl-pyridines, and pyridyl-azolate ligands.[2a,5c–e,g,6,9] The NHC ligands wider the HOMO–LUMO gap, compared to N-heterocycles, when coordinate to transition metals. Their π-acceptor ability effectively lowers the HOMO, whereas the strong σ-donor capacity raises the energy of the LUMO. For this reason, NHC ligands are particularly interesting to develop blue-emitting molecular osmium(II) complexes, which afford short lifetimes and narrow emission. This brings about better color purity and longer device lifetime. The most straight synthetic method to prepare transition-metal NHC complexes is direct metalation of azolium salts. This strategy requires the presence at the starting complex of a strong Brønsted base, which gives rise to labile ligands as a consequence of the deprotonation of the salts. Some neutral transition-metal polyhydride complexes have proven to be basic enough to cause the deprotonation of imidazolium and benzimidazolium salts, including the hexahydride complex **1**. However, products are highly dependent upon of the anion of the salt and the reaction solvent.
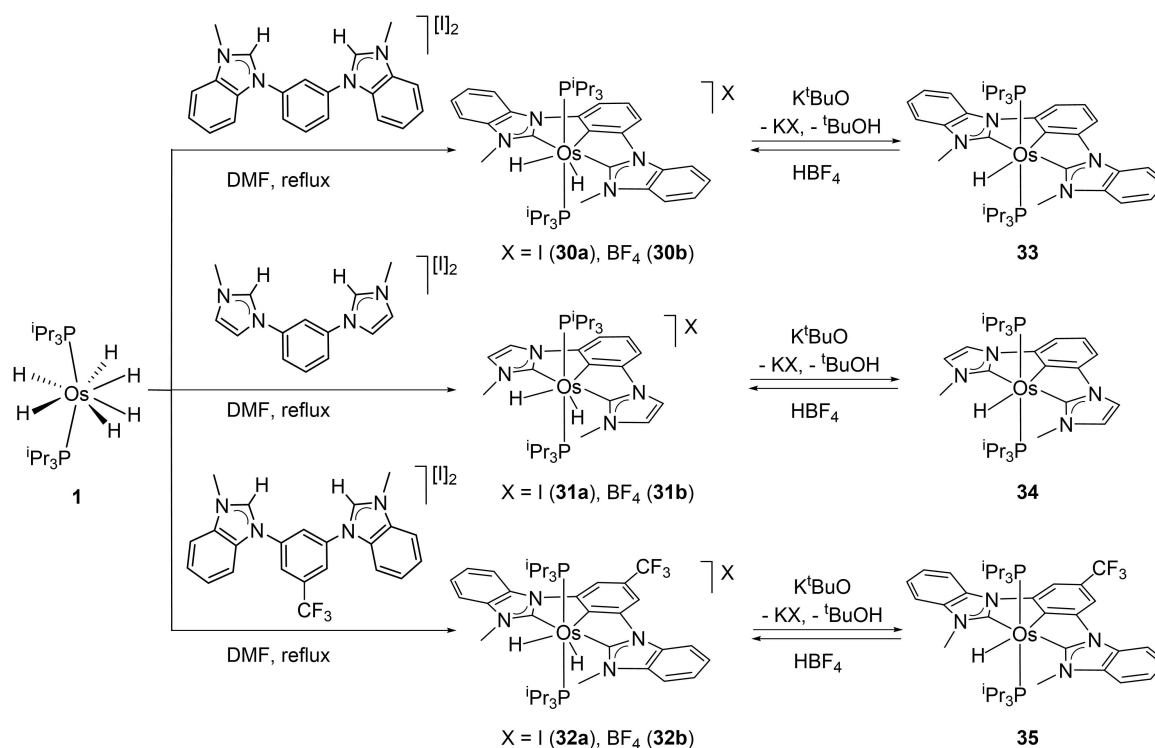
Treatment of dimethylformamide solutions of **1** with 1,3-bis (3-methylbenzimidazolium-1-yl)benzene tetrafluoroborate and 1,3-bis(3-methylimidazolium-1-yl)benzene tetrafluoroborate, under reflux, affords the osmium(II)-hydride-carbonyl complexes **28** and **29** (Scheme 7), resultant from a one-pot synthesis

Scheme 7. Preparation of complexes **28** and **29**.

involving three reactions, namely, direct metalation of one of the NHC groups of the salt, activation of the C–H bond at 6-position of the benzene linker, and metal carbonylation as a consequence of the solvent decarbonylation.[36]

The C–H bond activation of the benzene ring at the 6-position places the second benzimidazolium or imidazolium unit in a *para* position with respect to the metal center, preventing its metalation, while the activation at the 2-position is necessary for the coordination of the second NHC unit. The anion of the salt decides the position of the C–H bond of the linker that is broken and therefore the bidentate or tridentate nature of the resulting ligand. In contrast to the BF4-salts, the

EurJIC
European Journal of Inorganic Chemistry

Minireviews
doi.org/10.1002/ejic.202100663

Chemistry Europe
European Chemical Societies Publishing

Scheme 8. Preparation of complexes **30**–**35**.

iodide counterparts of 1,3-bis(3-methylbenzimidazolium-1-yl)benzene, 1,3-bis(3-methylimidazolium-1-yl)benzene, and 1,3-bis-(methylbenzimidazolium-1-yl)-5-trifluoromethylbenzene react with **1**, in dimethylformamide, under reflux to give the iodide salts of the pincer osmium(IV)-dihydride complexes **30a**–**32a** (Scheme 8), resultant from the C−H bond activation at the 2-position of the aryl linker and the metalation of both NHC units. Cations of these salts are quite acidic and can be easily deprotonated with K^{t}BuO, in tetrahydrofuran, to give the corresponding osmium(II)-monohydride derivatives **33**–**35**. The hydride abstraction is reversible. The addition of HBF$_4$ to the monohydrides causes the quantitative formation of the corresponding BF$_4$-salts **30b**–**32b**, which cannot be obtained through the direct reaction between **1** and the tetrafluoroborate azolium salts.

Homoleptic osmium(II) complexes bearing two *C,C',C*-pincer ligands have been synthesized from the corresponding osmium(II)-monohydride derivatives (Scheme 9). The reaction of **33** with 1,3-bis(3-methylbenzimidazolium-1-yl)benzene tetrafluoroborate and trimethylamine, in dimethylformamide, under reflux yields the neutral homoleptic complex **36**. Under identical conditions, the reaction of **35** with 1,3-bis(3-methylbenzimidazolium-1-yl)-5-trifluoromethylbenzene tetrafluoroborate leads to **37**.
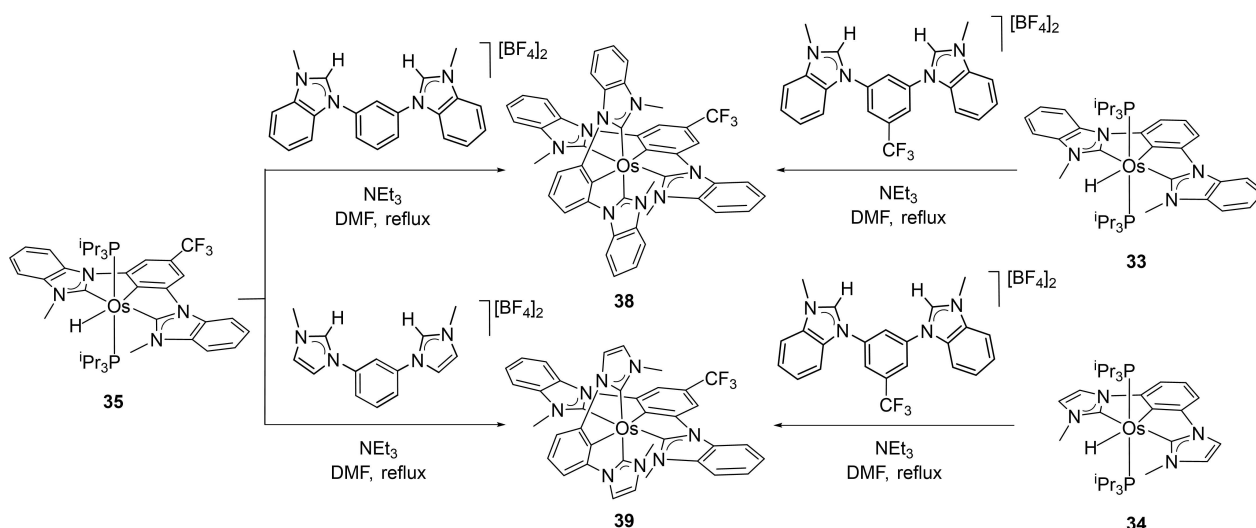
The monohydride complexes **33**–**35** also allow to synthesize heteroleptic osmium(II) emitters featuring two different *C,C',C*-pincer ligands (Scheme 10). Reaction of dimethylformamide solutions of **35** with 1,3-bis(3-methylbenzimidazolium-1-yl)benzene tetrafluoroborate and 1,3-bis-(methylimidazolium-1-
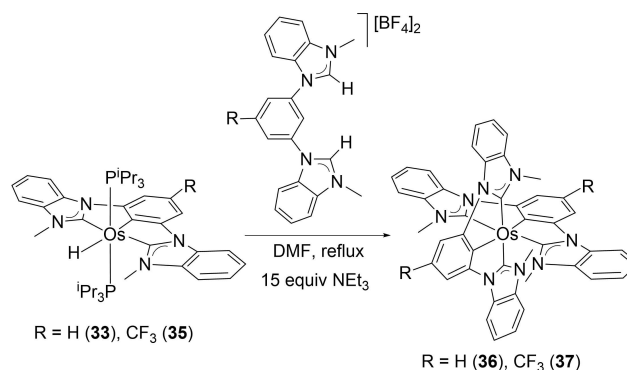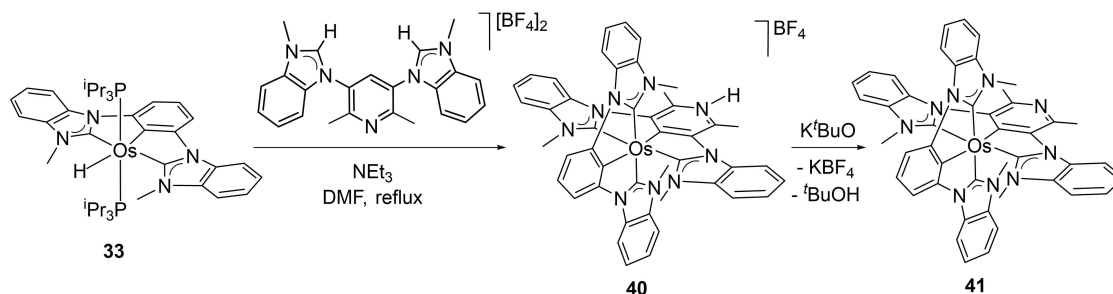

Scheme 9. Preparation of complexes **36** and **37**.

yl)benzene tetrafluoroborate, in the presence of trimethylamine (15 equiv), under reflux yields the heteroleptic derivatives **38** and **39** of the class [5t + 5t'], which can be also prepared starting from the respective monohydrides **33** and **34** and 1,3-bis(3-methylbenzimidazolium-1-yl)-5-trifluoromethyl benzene tetrafluoroborate.

This methodology is useful to prepare even heteroleptic [5t + 5t'] emitters containing an heterocyclic linker in one of the *C,C'C*-pincer ligands (Scheme 11). Under the standard conditions, the reaction of **33** with 3,5-bis(3-methylbenzimidazolium-1-yl)-2,6-dimethylpyridine tetrafluoroborate leads to **40**, which gives **41** by abstraction of the NH proton with K^{t}BuO, in tetrahydrofuran.

EurJIC
European Journal of Inorganic Chemistry

Minireviews
doi.org/10.1002/ejic.202100663

Chemistry
Europe
European Chemical
Societies Publishing

Scheme 10. Preparation of complexes **38** and **39**.

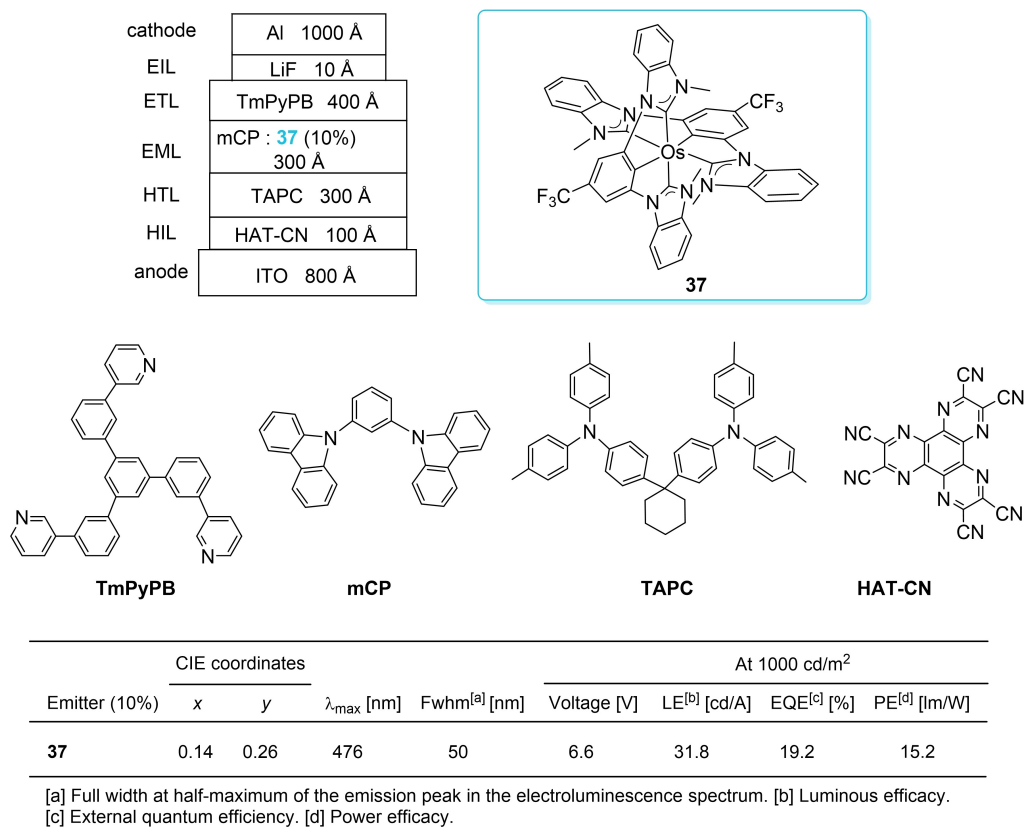**Scheme 11.** Preparation of complexes **40** and **41**.

Complexes **36**–**39** and **41** are phosphorescent emitters in the blue-green region (475–578 nm), in the solid state at 298 K and in toluene, at 298 and 77 K. Compound **37** displays light blue emission with a quite high quantum yield of 0.62. Therefore, it was selected as an emitter for the fabrication of a device. Figure 3 shows the structure of the device and summarizes its main characteristics at 1000 cd/m^2. The efficiency is comparable to that of modern iridium-based devices[10,17,37] The electroluminescence spectrum displays a peak at 476 nm with full width at half-maximum of 50 nm and CIE coordinates of (0.14, 0.26). The device starts to emit light at 3 V, while the brightness is 1000 cd/m^2 at 6.6 V, which becomes 10000 cd/m^2 at 9.5 V. At a brightness of 100 cd/m^2, the maximum power efficiency is 17 lm/W. The external quantum efficiency (EQE) is 19.2% at a luminance of 1000 cd/m^2 and the device keeps on highly efficient at higher brightness although significant efficiency roll-off was noticed at brightnesses > 10000 cd/m^2.[36]

The hexahydride complex **1** also promotes the metalation of the benzimidazolium units and the *ortho*-CH bond activation of the phenyl substituents of 1,1'-diphenyl-3,3'-ethylenedibenzi-mizazolium dibromide, in dimethyl sulfoxide, at 140°C. The multiple C—H bond activation leads to the bis(solvento)

compound **42**, bearing a dianionic *C,C',C,C'*-tetradentate ligand in a sawhorse-type coordination mode, with two *trans*-disposed phenyl groups and two *cis*-disposed NHC units (Scheme 12). The dimethyl sulfoxide molecules can be displaced by bidentate ligands to afford osmium(II) emitters of the class [6tt + 4b]. Compound **42** reacts with the diphosphines 1,2-bis-(diphenyl-phosphino)ethylene and 1,2-bis(diphenylphosphino)benzene, in tetrahydrofuran, to yield **43** and **44**, respectively. During the reactions, a change in the disposition of the donor atoms of the tetradentate ligand takes place. In contrast to that observed for **42**, the phenyl groups of **43** and **44** are mutually *cis*-oriented. Complex **44** is emissive in the orange region (550–600 nm) with a photoluminescence quantum yield of 0.05 in PMMA film.[38]

Compounds related to **44**, bearing two free phenylbenzimi-dazolylidene groups, were also prepared to gain insight into the influence of the ethylene linker on the disposition of the donor atoms of the tetradentate ligand and on the photo-physical properties. They were obtained according to Scheme 13, starting from the tetrakis(solvento) complexes **45** and **46** via a two steps procedure.[39] These compounds initially react with 1,2-bis-(diphenylphosphino)benzene in dichlorome-thane to afford **47** and **48**. The subsequent treatment of dimethylformamide solutions of **47** and **48** with the iodide salts

EurJIC
European Journal of Inorganic Chemistry

Minireviews
doi.org/10.1002/ejic.202100663

Chemistry Europe
European Chemical
Societies Publishing

cathode	Al 1000 Å
EIL	LiF 10 Å
ETL	TmPyPB 400 Å
EML	mCP : **37** (10%) 300 Å
HTL	TAPC 300 Å
HIL	HAT-CN 100 Å
anode	ITO 800 Å

TmPyPB **mCP** **TAPC** **HAT-CN**

	CIE coordinates				At 1000 cd/m^2			
Emitter (10%)	x	y	λ_{max} [nm]	Fwhm[a] [nm]	Voltage [V]	LE[b] [cd/A]	EQE[c] [%]	PE[d] [lm/W]
37	0.14	0.26	476	50	6.6	31.8	19.2	15.2

[a] Full width at half-maximum of the emission peak in the electroluminescence spectrum. [b] Luminous efficacy.
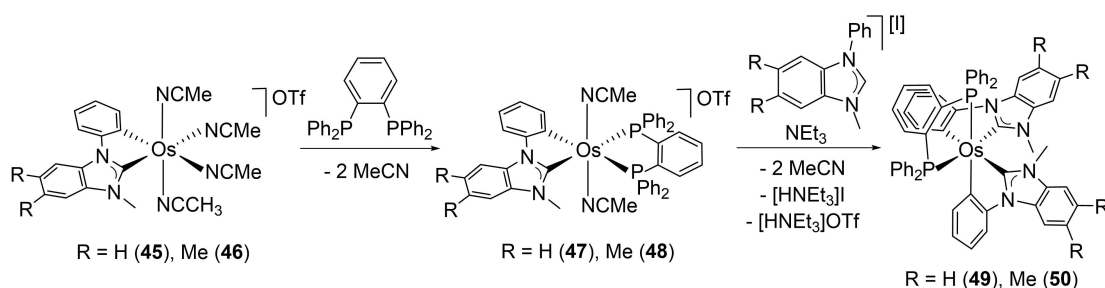[c] External quantum efficiency. [d] Power efficacy.

Figure 3. Structure and performance data of the device based on complex **37**. Abbreviations: HIL, hole-injector layer; HTL, hole-transporting layer; EML, emissive layer; ETL, electron-transporting layer; EIL, electron-injector layer.
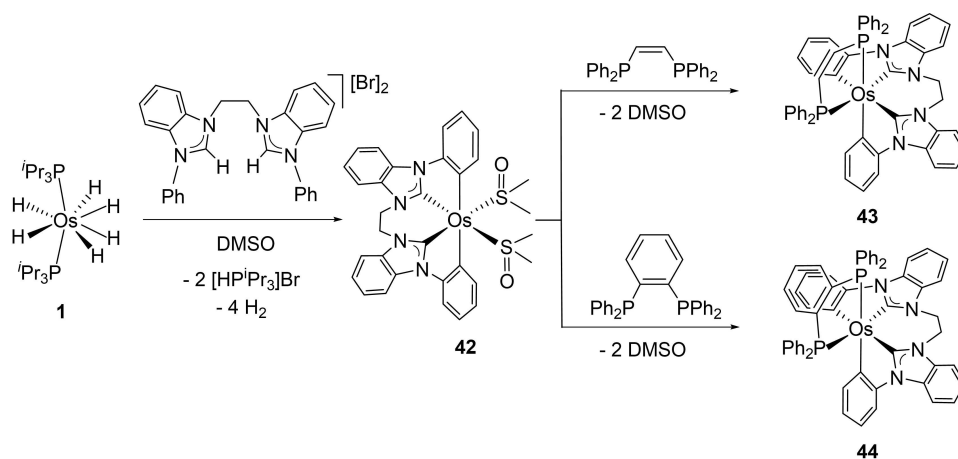
Scheme 12. Preparation of complexes **43** and **44**.

of 1-phenyl-3-methyl-1*H*-benzimidazolium and 1-phenyl-3-methyl-1*H*-5,6-dimethyl-benzimidazolium, in the presence of 10 equiv. of triethylamine, at 110 °C produces the substitution of the remaining acetonitrile molecules, by the corresponding orthometalated benzimidazolylidene ligand, to generate **49** and **50** with the same disposition for the donor atoms as **44**; i.e., the —CH$_2$CH$_2$— chain does not decide the structure of the latter. Complexes **49** and **50** also exhibit orange emission (600–

630 nm) with a quantum yield of 0.05 in PMMA film. A deeper comparison of the spectra indicates that the —CH$_2$CH$_2$— chain favors narrower and bluer emissions.[38]

EurJIC
European Journal of Inorganic Chemistry

Minireviews
doi.org/10.1002/ejic.202100663

Chemistry
Europe
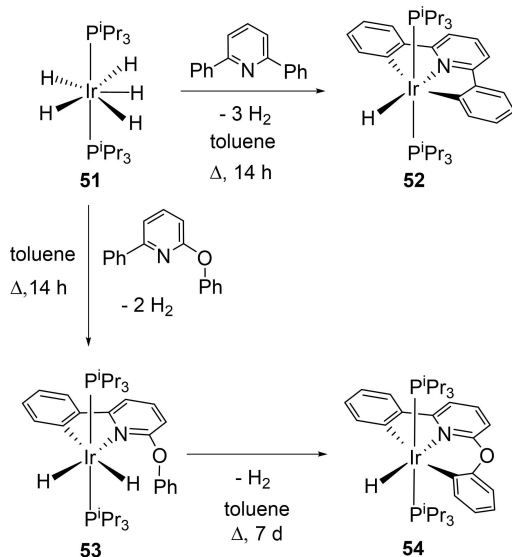European Chemical
Societies Publishing

Scheme 13. Preparation of complexes **47–50**.

3. Iridium(III) Emitters

The value and usefulness of the hexahydride complex **1** as starting material to the preparation of phosphorescent emitters is not an inherent property of this compound or even of the element. It is related to its polyhydride character and the ability of complexes of platinum group metals of this class, to activate σ-bonds. Such ability is also manifested in the iridium pentahydride **51**. Thus, in agreement with **1**, complex **51** promotes the activation of an *ortho*-CH bond of both substituents of the pyridines 2,6-diphenylpyridine and 2-phenoxy-6-phenylpyridine (Scheme 14), being the orthometalation of phenyl much quicker than that of phenoxide. Treatment of **51** with 2,6-diphenylpyridine, in toluene, under reflux gives the iridium(III) monohydride complex **52**, after 14 h. Under the same conditions, the activation of both substituents of 2-phenoxy-6-phenylpyridine takes place after one week in a sequential manner. The phenyl activation gives the dihydride intermediate **53**, which evolves to the double activation product **54** releasing a hydrogen molecule.

Complex **52** is a moderate phosphorescent emitter (Table 1), which exhibits green emission (540 nm) with a quantum yield of 0.21, in PMMA film at 5 wt%. In 2-MeTHF solution, the emission is red shifted (601 nm at 298 K and 581 nm at 77 K), while the quantum yield remains (0.23). In contrast to that observed for the osmium compounds **21** and **22**, the incorporation of the oxygen atom causes a significant blue shift of the emission and a notable increase in the efficiency of the emitter. Therefore, complex **54** displays green-blue emission (538–473 nm), with quantum yields of 0.87 in PMMA film at 5 wt% and 0.96 in 2-MeTHF at 298 K.[34]

The comparison of the iridium(III) derivatives **52** and **54** with the osmium(IV) counterparts **21** and **22** emphasizes the crucial role of the bite angle of pincer ligands on the photophysical features of these emitters. The emissions are attributed to T_1 excited states. Their geometries largely depend on the presence of the oxygen atom between the pyridine ring and a phenyl group. While for iridium(III) it favors the octahedral geometry of the T_1 state, since the phenoxy-iridium-pyridine angle is close to the ideal of 90°, for osmium(IV) it disfavors the pentagonal-bipyramidal arrangement of the T_1 state due to the deviation of the phenoxy-osmium-pyridine angle from the ideal of 72°.

Coherent synthetic methods for the preparation of phosphorescent heteroleptic iridium(III) emitters of the class [3b+3b'+2m+1m'], based on 2-phenylquinoline and acetylacetonate (acac), with controlled stereochemistry, have also been developed starting from the pentahydride **51** (Scheme 15 and Scheme 16).[40]

Complex **51** activates an *ortho*-CH bond of the phenyl substituent of 2-phenylquinoline to give the dihydride derivative **55**. This compound acts as a Brønsted base. So, its reaction with HBF₄ causes the release of molecular hydrogen, as a consequence of the protonation of a basic hydride, and the formation of salt **56**. The reaction of the five-coordinate monohydride cation with Kacac produces the displacement of one of the phosphines and the coordination of the *O,O*-chelate to regioselectively form the six-coordinate molecular monohydride **57** (Scheme 15)

Complex **56** allows to prepare alkenyl derivatives related to **57** in two steps, namely, alkyne insertion and successive acac coordination. Its unsaturated character enables the insertion of the C–C triple bond of terminal alkynes into the Ir–H bond. Thus, the reactions of **56** with phenylacetylene and acetylene afford the five-coordinate styryl (**58**) and vinyl (**59**) derivatives, respectively. Complexes **58** and **59** react with Kacac to afford

Scheme 14. Preparation of complexes **52–54**.

EurJIC
European Journal of Inorganic Chemistry

Minireviews
doi.org/10.1002/ejic.202100663

Chemistry
Europe
European Chemical
Societies Publishing
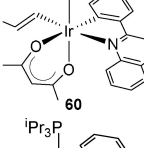
Table 1. Photophysical properties of the iridium(III) emitters.
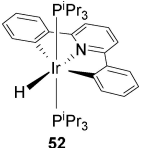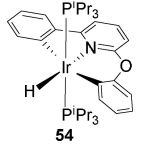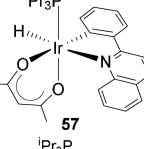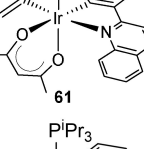
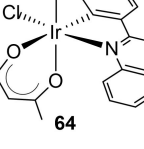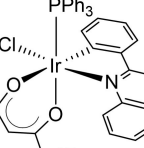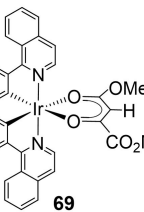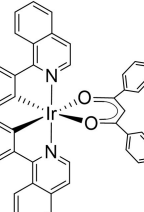| Complex	HLG[a] [eV]	Emission color	Medium	λ_{em} [nm]	τ [µs]	Φ	$k_r^{[b]}$ [s^{-1}]	$k_{nr}^{[c]}$ [s^{-1}]	Ref.
52	3.83	green	PMMA-298K	540	0.6	0.21	3.5×10^5	1.3×10^6	34
			2-MeTHF-298K	601	0.3	0.23	7.7×10^5	2.6×10^6	
			2-MeTHF-77K	581	5.2				
54	3.83	green-blue	PMMA-298K	481, 513	1.5	0.87	5.8×10^5	8.7×10^4	34
			2-MeTHF-298K	482, 515	2.0	0.96	4.8×10^5	2.0×10^4	
			2-MeTHF-77K	473, 509, 538	6.7				
57	3.35	yellow	PMMA-298K	575	1.2	0.75	6.3×10^5	2.1×10^5	40
			2-MeTHF-298K	562	0.6				
			2-MeTHF-77K	525, 564	6.6				
60	2.82	yellow-orange	PMMA-298K	581	1.4	0.04	2.9×10^4	6.9×10^5	40
			2-MeTHF-298K	592	0.6				
			2-MeTHF-77K	535, 570	5.7				
61	3.21	yellow	PMMA-298K	570, 606	1.9	0.64	3.4×10^5	1.9×10^5	40
			2-MeTHF-298K	577	0.8				
			2-MeTHF-77K	526, 564	4.0				
64	3.28	orange	PMMA-298K	613	1.2	0.27	2.3×10^5	6.0×10^5	40
			2-MeTHF-298K	605	1.4				
			2-MeTHF-77K	551, 591	3.1				
65	3.64	yellow	PMMA-298K	565	1.8	0.28	1.5×10^5	4.0×10^5	40
			2-MeTHF-298K	584	2.8				
			2-MeTHF-77K	536, 573	6.0				
69	3.18	red	PMMA-298K	619, 665	1.1	0.52	4.7×10^5	4.4×10^5	41
			2-MeTHF-298K	622, 667	1.4	0.62	4.4×10^5	2.7×10^5	
			2-MeTHF-77K	599, 653, 712	2.5				
70	3.13	red	PMMA-298K	638, 670	1.0	0.32	3.2×10^5	6.8×10^5	41
			2-MeTHF-298K	628, 668	0.8	0.35	4.4×10^5	2.7×10^5	
			2-MeTHF-77K	608, 658, 723	2.4				

EurJIC
European Journal of Inorganic Chemistry

Minireviews
doi.org/10.1002/ejic.202100663

Chemistry
Europe
European Chemical
Societies Publishing

Table 1. continued
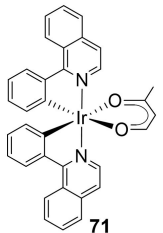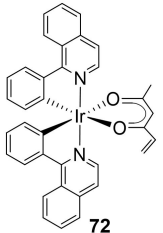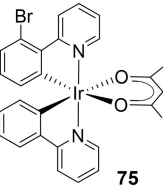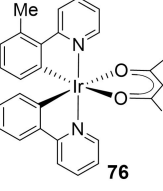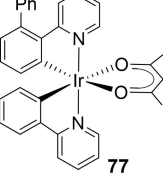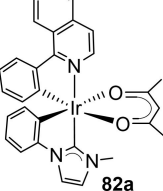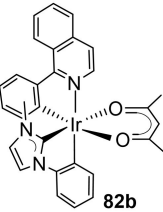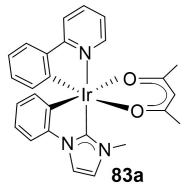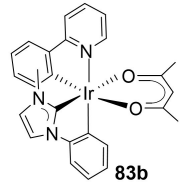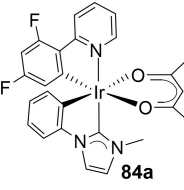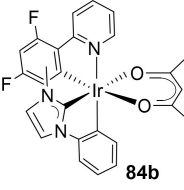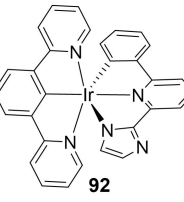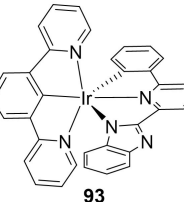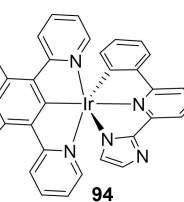
Complex	HLG[a] [eV]	Emission color	Medium	λ_{em} [nm]	τ [µs]	Φ	$k_r^{[b]}$ [s^{-1}]	$k_{nr}^{[c]}$ [s^{-1}]	Ref.
71	3.17	red	PMMA-298K 2-MeTHF-298K 2-MeTHF-77K	626, 669 627, 668 605, 659, 719	0.9 1.2 2.5	0.50 0.52	5.6×10^5 4.3×10^5	5.6×10^5 4.0×10^5	41
72	3.16	red	PMMA-298K 2-MeTHF-298K 2-MeTHF-77K	642, 672 641 617, 672, 733	0.9 1.3 2.1	0.31 0.35	3.4×10^5 2.7×10^5	7.6×10^5 5.0×10^5	41
75	3.59	green	PMMA-298K 2-MeTHF-298K 2-MeTHF-77K	527 528 511, 548, 596	0.4 1.0 5.6	0.32 0.41	9.0×10^5 3.9×10^5	1.9×10^6 5.6×10^5	44
76	3.62	green	PMMA-298K 2-MeTHF-298K 2-MeTHF-77K	526 527 509, 547, 594	0.9 1.8 4.9	0.82 0.86	9.4×10^5 4.8×10^5	2.1×10^5 7.9×10^4	44
77	3.61	green	PMMA-298K 2-MeTHF-298K 2-MeTHF-77K	529 529 512, 550, 597	0.6 1.7 5.4	0.84 0.98	1.4×10^6 5.6×10^5	2.7×10^5 1.2×10^4	44
82a	3.16	red	PMMA-298K 2-MeTHF-298K 2-MeTHF-77K	652 619 597, 652	1.3 1.8 3.3	0.70 0.93	5.4×10^5 5.2×10^5	2.3×10^5 3.9×10^4	46
82b	3.15	red	PMMA-298K 2-MeTHF-298K 2-MeTHF-77K	629 618 580, 623	1.3 1.8 3.3	0.71 0.78	5.5×10^5 4.3×10^5	2.2×10^5 1.2×10^5	46

EurJIC
European Journal of Inorganic Chemistry

Minireviews
doi.org/10.1002/ejic.202100663

Chemistry Europe
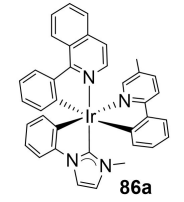European Chemical
Societies Publishing

Table 1. continued

Complex	HLG[a] [eV]	Emission color	Medium	λ_{em} [nm]	τ [µs]	Φ	k_r[b] [s^{-1}]	k_{nr}[c] [s^{-1}]	Ref.
83a	3.66	green	PMMA-298K	510	1.5	0.86	5.7×10^5	9.3×10^4	46
			2-MeTHF-298K	516	1.4	0.67	4.8×10^5	2.4×10^5	
			2-MeTHF-77K	495, 532	5.0				
83b	3.70	green	PMMA-298K	498	1.3	0.77	5.9×10^5	1.8×10^5	46
			2-MeTHF-298K	505	1.1	0.90	8.2×10^5	9.1×10^4	
			2-MeTHF-77K	484, 517	4.1				
84a	3.75	green	PMMA-298K	495	1.1	0.87	7.9×10^5	1.2×10^5	46
			2-MeTHF-298K	494	0.2	0.56	2.8×10^6	2.2×10^6	
			2-MeTHF-77K	475, 506	5.6				
84b	3.77	green	PMMA-298K	497	1.0	0.72	7.4×10^5	2.9×10^5	46
			2-MeTHF-298K	489	0.6	0.74	1.3×10^6	4.3×10^5	
			2-MeTHF-77K	465. 496	3.9				
86a	3.15	red	PMMA-298K	636	0.2	0.34	1.7×10^6	3.3×10^6	46
			2-MeTHF-298K	632	0.9	0.40	4.4×10^5	6.7×10^5	
			2-MeTHF-77K	606, 637	2.7				
92	3.49	green	PMMA-298K	510, 541	1.2	0.37	3.1×10^5	5.3×10^5	50
			2-MeTHF-298K	512, 547	0.8	0.35	4.4×10^5	8.1×10^5	
			2-MeTHF-77K	503, 542	9.7				
93	3.54	green	PMMA-298K	514, 541	0.5	0.40	8.0×10^5	1.2×10^6	50
			2-MeTHF-298K	514, 547	0.6	0.37	6.2×10^5	1.1×10^6	
			2-MeTHF-77K	502, 540	8.8				
94	3.57	green	PMMA-298K	509, 534	2.5	0.61	2.4×10^5	1.6×10^5	50
			2-MeTHF-298K	506, 540	1.4	0.64	4.6×10^5	2.6×10^5	
			2-MeTHF-77K	491, 529	2.5				

EurJIC
European Journal of Inorganic Chemistry

Minireviews
doi.org/10.1002/ejic.202100663

Chemistry Europe
European Chemical
Societies Publishing

Table 1. continued
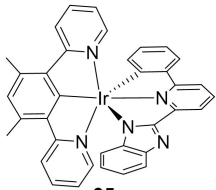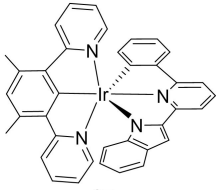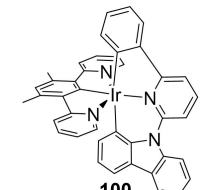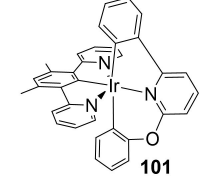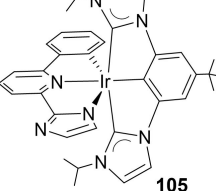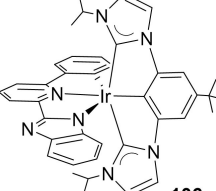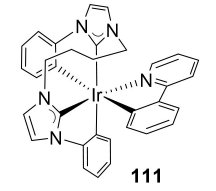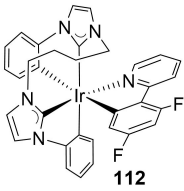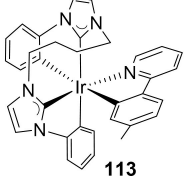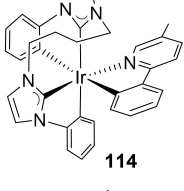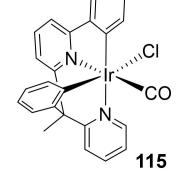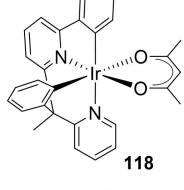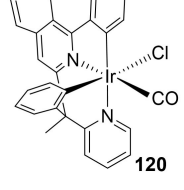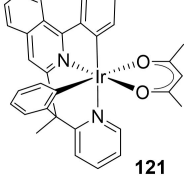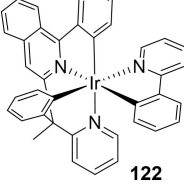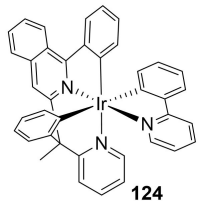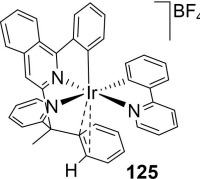
Complex	HLG[a] [eV]	Emission color	Medium	λ_{em} [nm]	τ [μs]	Φ	k_r[b] [s^{-1}]	k_{nr}[c] [s^{-1}]	Ref.
95	3.61	green	PMMA-298K	508, 535	2.1	0.68	3.2×10^5	1.5×10^5	50
			2-MeTHF-298K	507, 538	1.5	0.52	3.5×10^5	3.2×10^5	
			2-MeTHF-77K	493, 532	3.6				
97	3.30	green-yellow	PMMA-298K	564, 609	2.5	0.30	1.2×10^5	2.8×10^5	50
			2-MeTHF-298K	576, 624	1.3	0.20	1.5×10^5	6.2×10^5	
			2-MeTHF-77K	547, 594	3.0				
100	3.47	green	PMMA-298K	528	2.1	0.73	3.5×10^5	1.3×10^5	52
			2-MeTHF-298K	555	2.0				
			2-MeTHF-77K	515, 548	10.1				
101	3.55	green	PMMA-298K	524	1.3	0.87	6.7×10^5	1.0×10^5	52
			2-MeTHF-298K	539	7.7				
			2-MeTHF-77K	516, 545	5.9				
105	3.84	green	PMMA-298K	490, 525, 560	2.1	0.73	3.5×10^5	1.3×10^5	55
			2-MeTHF-298K	496, 531, 567	1.2	0.60	5.0×10^5	3.3×10^5	
			2-MeTHF-77K	482, 520, 550	5.9				
106	3.70	yellow-green	PMMA-298K	590	4.1	0.49	1.2×10^5	1.2×10^5	55
			2-MeTHF-298K	542	4.1	0.56	1.4×10^5	1.1×10^5	
			2-MeTHF-77K	506, 543, 585	11.7				
111	3.76	green	PMMA-298K	509	1.7	0.93	5.5×10^5	4.1×10^4	56
			2-MeTHF-298K	510	3.9	~1	2.6×10^5		
			2-MeTHF-77K	478, 506	4.8				

EurJIC
European Journal of Inorganic Chemistry

Minireviews
doi.org/10.1002/ejic.202100663

Chemistry Europe
European Chemical
Societies Publishing

Table 1. continued

Complex	HLG[a] [eV]	Emission color	Medium	λ_{em} [nm]	τ [μs]	Φ	k_r[b] [s^{-1}]	k_{nr}[c] [s^{-1}]	Ref.
112	3.81	blue-green	PMMA-298K	485	1.3	0.87	6.7×10^5	1.0×10^5	56
			2-MeTHF-298K	473	1.6	0.73	4.6×10^5	1.7×10^5	
			2-MeTHF-77K	455, 484	3.1				
113	3.79	green	PMMA-298K	509	1.7	0.93	5.5×10^5	4.1×10^4	56
			2-MeTHF-298K	492	3.1	~1	3.2×10^5		
			2-MeTHF-77K	473, 506	4.5				
114	3.78	green	PMMA-298K	508	1.8	0.96	5.3×10^5	2.2×10^4	56
			2-MeTHF-298K	492	2.4	~1	4.2×10^5		
			2-MeTHF-77K	476, 510	4.4				
115	3.98	blue-green	PMMA-298K	474, 502	1.1	0.87	7.6×10^5	1.1×10^5	59
			2-MeTHF-298K	478, 508, 541	2.0	0.54	2.7×10^5	2.3×10^5	
			2-MeTHF-77K	468, 503, 534	2.9				
118	3.71	green	PMMA-298K	551	2.2	0.71	3.3×10^5	1.4×10^5	59
			2-MeTHF-298K	552	2.3	0.66	2.8×10^5	1.4×10^5	
			2-MeTHF-77K	527, 562	4.5				
120	3.61	red	PMMA-298K	645	1.4	0.08	5.7×10^4	6.6×10^5	62
			2-MeTHF-298K	645	2.6	0.13	5.0×10^4	3.4×10^5	
			2-MeTHF-77K	601, 647	3.8				
121	3.27	red	PMMA-298K	681	0.7	0.57	8.1×10^5	6.1×10^5	62
			2-MeTHF-298K	682	0.8	0.58	7.4×10^5	5.3×10^5	
			2-MeTHF-77K	665, 715	1.2				
122	3.13	red	PMMA-298K	679, 720	0.9	0.17	1.9×10^5	9.2×10^5	62
			2-MeTHF-298K	676	1.5	0.25	1.7×10^5	5.0×10^5	
			2-MeTHF-77K	650, 701	1.8				

EurJIC
European Journal of Inorganic Chemistry

Minireviews
doi.org/10.1002/ejic.202100663

Chemistry Europe
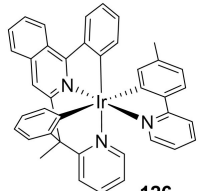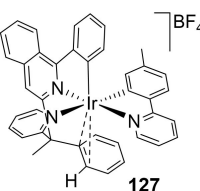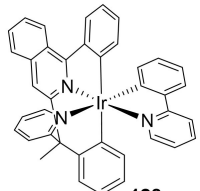European Chemical
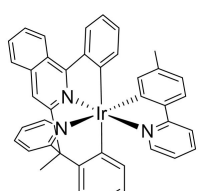Societies Publishing

Table 1. continued

Complex	HLG[a] [eV]	Emission color	Medium	λ_{em} [nm]	τ [μs]	Φ	$k_r^{[b]}$ [s^{-1}]	$k_{nr}^{[c]}$ [s^{-1}]	Ref.
124	3.16	red	PMMA-298K	663	1.2	0.29	2.4×10^5	5.9×10^5	62
			2-MeTHF-298K	668	2.3	0.22	9.6×10^5	3.4×10^5	
			2-MeTHF-77K	646, 699	1.3				
125	3.35	red	PMMA-298K	669	1.4	0.18	1.3×10^5	5.9×10^5	62
			2-MeTHF-298K	663	1.6	0.17	1.1×10^5	5.2×10^5	
			2-MeTHF-77K	617, 647	2.7				
126	3.14	red	PMMA-298K	663	1.6	0.23	1.4×10^5	4.8×10^5	62
			2-MeTHF-298K	668	1.5	0.38	2.5×10^5	4.1×10^5	
			2-MeTHF-77K	649, 698	2.2				
127	3.32	red	PMMA-298K	678	1.2	0.16	1.3×10^5	7.0×10^5	62
			2-MeTHF-298K	666	1.8	0.19	1.1×10^5	4.5×10^5	
			2-MeTHF-77K	608, 652	3.6				
128	3.05	red	PMMA-298K	694, 715	4.6	0.16	3.5×10^4	1.8×10^5	62
			2-MeTHF-298K	692	2.0	0.12	6.0×10^4	4.4×10^5	
			2-MeTHF-77K	668, 709	1.3				
129	3.04	red	PMMA-298K	681	2.1	0.13	6.2×10^4	4.1×10^5	62
			2-MeTHF-298K	732	1.4	0.14	1.0×10^5	4.4×10^5	
			2-MeTHF-77K	671, 729	1.5				

[a] DFT-calculated HOMO–LUMO gap. [b] $k_r = \Phi/\tau$. [c] $k_{nr} = (1-\Phi)/\tau$.

the neutral alkenyl species **60** and **61**, in a similar manner to their hydride precursor **56** (Scheme 16).

Chloride compounds related to **57**, **60**, and **61**, were synthesized through *cis*-dichloride intermediates **62** and **63** (Scheme 17). These five-coordinate species were prepared by consecutive addition of 1 equiv. of the corresponding phosphine and 1 equiv. of 2-phenylquinoline to IrCl$_3$(tht)$_3$ in refluxing decalin. Complexes **62** and **63** react with Kacac, under the same conditions as **56**, **58**, and **59**, to yield **64** and **65**.

Complexes **57**, **60**, **61**, **64**, and **65** display yellow-orange emission (613–525 nm), when photoexcited, in PMMA film at 5 wt% at 298 K and 2-MeTHF at 298 and 77 K. The observed lifetimes are in the range of 0.6–6.6 μs, while the quantum yields in the film vary between 0.75 and 0.04 (Table 1). The monodentate ligand has little effect on the color, with the emission showing a slight change from yellow to orange in the order H < CH=CH$_2$ < CH=CHPh < Cl. On the contrary, the quantum yields display marked dependence on the mono-

EurJIC
European Journal of Inorganic Chemistry

Minireviews
doi.org/10.1002/ejic.202100663

Chemistry Europe
European Chemical
Societies Publishing
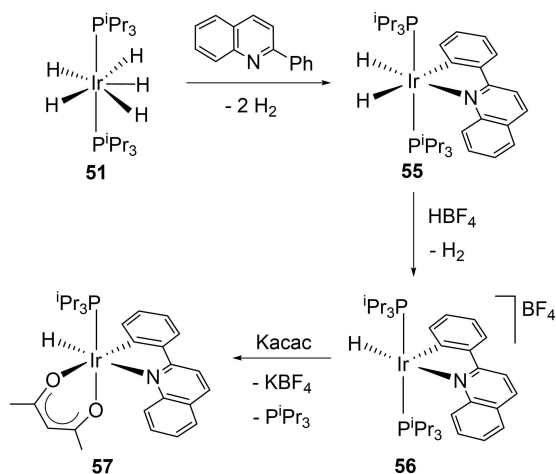
Scheme 15. Preparation of complexes 55–57.
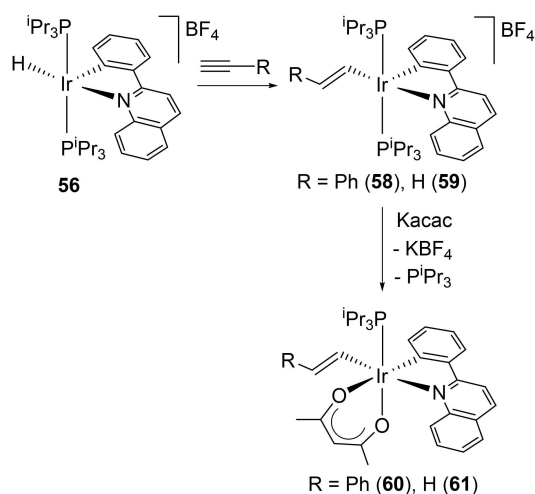
Scheme 16. Preparation of complexes 58–61.

Scheme 17. Preparation of complexes 62–65.

dentate ligand, increasing in the order CH=CHPh < Cl < CH=CH₂ < H.

A new methodology of synthesis to generate, on the metal coordination sphere, emitters with an asymmetrical β-diketonate ligand was developed in 2020. The procedure should facilitate a better adjustment on the emissive properties of β-diketonate-containing emitters, given the wide variety of substituents that can be introduced at the carbonyl groups. The procedure involves the addition of the O–H bond of iridium(III)-

hydroxo compounds across the activated C–C multiple bond of alkynes and olefins bearing carbonyl substituents, in accordance with the hydroxoacid nature of this type of transition metal species.[41]

The methodology was optimized using orthometalated 1-phenylisoquinoline as chromophore and was stimulated by earlier studies on the d^6-pentacoordinate osmium(II) compounds OsH(XH)(CO)(P^{i}Pr$_3$)$_2$ (XH=OH, SH), which in the presence of dimethyl acetylenedicarboxylate afford OsH{κ^2-X,O-[XC-(CO$_2$CH$_3$)CHC(OCH$_3$)O]}(CO)(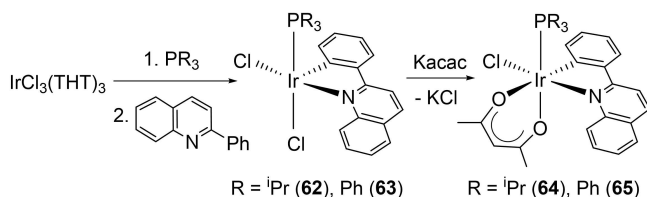P^{i}Pr$_3$)$_2$ (X=O,[42] S[43]). It was thought that an iridium system [Ir(OH)(3b)$_2$], where the 3b unit is an orthometalated 1-phenylisoquinoline, should show similar reactivity to the osmium(II) complexes, because both iridium and osmium are third row platinum group metals and such iridium fragment also contains a d^6-unsaturated metal center. The dimeric complexes [Ir(μ-OH)(3b)$_2$]$_2$ are the stable form of the unsaturated [Ir(OH)(3b)$_2$] counterparts. The hydroxide dimeric complex containing orthometalated 1-phenylisoquinoline was prepared according to Scheme 18. Treatment of acetone solutions of the dinuclear chloride-bridged complex [Ir(μ-Cl)(3b)$_2$]$_2$ 66 with AgBF$_4$ followed by filtration, to remove the AgCl, and addition of water gives the bis(aquo) mononuclear complex 67. The coordination of the water molecules to the acidic iridium center of 67 increases the Brønsted acidity of these ligands, enabling their deprotonation. Accordingly, the reaction of acetone solutions of 67 with KOH affords the desired hydroxo-bridged dinuclear complex 68. Although maintaining the *N,N-trans* orientation, both racemic and *meso* isomers are possible, only the less sterically congested enantiomeric pair is selectively formed. In agreement with this, DFT calculations indicate that the enantiomers are 14.8 kcal mol⁻¹ more stable than the *meso* form.
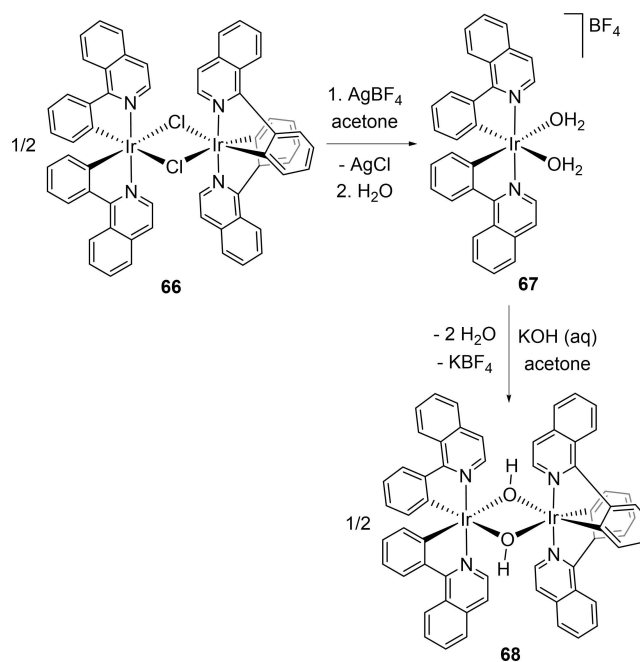
Scheme 18. Preparation of complexes 67 and 68.

EurJIC
European Journal of Inorganic Chemistry

Minireviews
doi.org/10.1002/ejic.202100663

Chemistry Europe
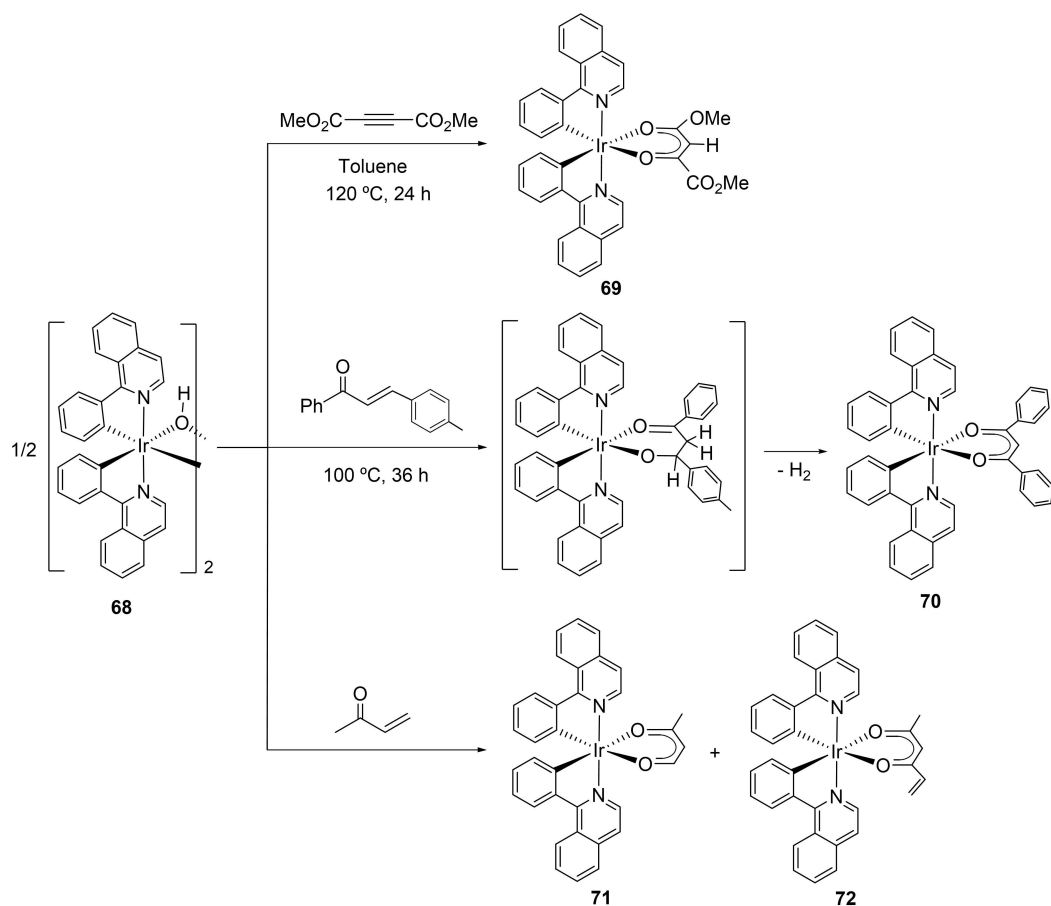European Chemical
Societies Publishing

Reaction of **68** with dimethyl acetylenedicarboxylate in toluene at 120 °C leads to **69**, as a consequence of the *trans*-insertion of the C—C triple bond of the alkyne into the O—H bond and the coordination of one of the carboxylate substituents to the iridium center (Scheme 19). The C—C double bond of 3-(4-methylphenyl)-1-phenylprop-2-en-1-one similarly inserts into the O—H bonds of **68** to give at first a dihydro-β-diketonate intermediate, resulting of a regioselective addition (H to C_α and O to C_β). The dihydro-β-diketonate group of this intermediate rapidly eliminates molecular hydrogen to yield **70**. The aromatization of the *O,O*-bidentate ligand seems to be the driving force to the formation of the asymmetrical β-diketonate. Methyl vinyl ketone also reacts with **68** in a similar manner to the previous unsaturated ketone to give **71**. However, in this case the reaction affords an additional compound **72** bearing a new asymmetrical β-diketonate ligand. The formation of the latter can be explained as follows: the basic nature of the OH group induces the condensation of two molecules of the ketone with elimination of one molecule of ethylene to give hex-5-ene-2,4-dione, which protonates the bridges of **68** and coordinates to the iridium center.

Complexes **69**–**72** are red phosphorescent emitters (Table 1). The substituents of the β-diketonate ligands have an insignificant effect on the emission color, which appears in the 599–672 nm range. This is consistent with almost equal DFT-calculated HOMO–LUMO energy gaps (3.13–3.18 eV). The observed lifetimes are between 0.8–2.5 µs. As opposed to the emission color, the quantum yields display marked dependence on the substituents of the β-diketonate ligand, in both PMMA film and 2-MeTHF. Particularly noticeable are those of complex **69**, containing an electron releasing methoxy substituent and an electron accepting carboxylate group (0.62 in 2-MeTHF and 0.52 in 5 wt% PMMA film), and complex **71**, which contains only a methyl substituent (0.52 in 2-MeTHF and 0.50 in 5 wt% PMMA film).[41]

Heteroleptic iridium(III) emitters of the type [3b+3b′+3b′′] have been recently prepared, by an elegant procedure, in twice the yield expected for the usual one-pot procedure. The novel complexes bear an orthometalated 2-phenylpyridine substituted on the phenyl at the *ortho* position with respect to the pyridyl (Scheme 20). The procedure is noteworthy not only by the yields afforded but also because it allows to study the influence of the substituents, at this elusive position, of the chromophore on the photophysical properties of the emitters.[44]

Dimers [Ir(μ-Cl)(η^2—COE)$_2$]$_2$ (**73**, COE = cyclooctene) and [Ir-(μ—Cl)(η^4—COD)]$_2$ (**74**, COD = 1,5-cyclooctadiene) activate *ortho*-C—H and *ortho*-C—Br bonds of the phenyl ring of 2-(2-bromophenyl)pyridine in a competitive way. The selectivity of the reactions is directed by the olefin of the precursor dimer

Scheme 19. Preparation of complexes **69**–**72**.

EurJIC
European Journal of Inorganic Chemistry

Minireviews
doi.org/10.1002/ejic.202100663

Chemistry Europe
European Chemical Societies Publishing
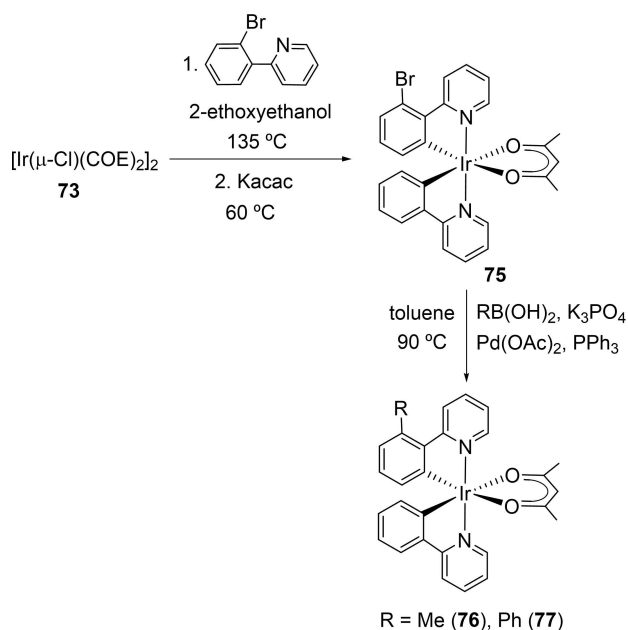
Scheme 20. Preparation of complexes **75–77**.

and the experimental conditions.[45] The cyclooctene dimer **73**, in 2-ethoxyethanol at 135 °C, induces the two cleavages in the same extension. Therefore, the tris-heteroleptic complex **75** bearing two different orthometalated 2-phenylpyridines, one of them with the phenyl ring brominated at an *ortho* position with

respect to the N-heterocycle, is selectively formed in high yield (82%). In spite of the steric hindrance, the brominated position was post-functionalized by Suzuki-Miyaura cross-coupling using RB(OH)$_2$ (R=Me, Ph) in the presence of Pd(OAc)$_2$/4 PPh$_3$ (10 mol%) and K$_3$PO$_4$. The resulting emitters **76** and **77** were isolated as pure yellow solids in a total yield of approximately 60% relative to the precursor **73**, after column chromatography.

Complexes **75–77** display green phosphorescence (509–597 nm, Table 1). The substituent of the phenyl group does not affect the emission color; the spectra of the three compounds being almost the same. However, the quantum yield is substituent-dependent. Thus, the replacement of the bromide of **75** by a methyl or phenyl group increases the efficiency of the emissive compound between 2 and 3 times. Thus, the heteroleptic derivatives **76** and **77** exhibit very high quantum yields between 0.98–0.82, in both PMMA films and 2-MeTHF.[44]

Heteroleptic dimers of the class [Ir(μ-Cl)(3b)(3b')]$_2$ containing an orthometalated 1-phenyl-3-methylimidazolylidene (PhMeIm) ligand, which allows an easy access to [3b + 3b' + 3b''] heteroleptic emitters, have been prepared in high yield by a direct procedure (Scheme 21).[46] The NHC ligand was initially coordinated to the iridium center of dimer **74** through transmetalation from the silver-NHC complex (PhMeIm)AgI, which was generated in situ. The transmetalation gives the square-planar mononuclear compound **78**, which was isolated in 92% yield. Complex **78** reacts with aryl-N-heterocycles such as 1-phenylisoquinoline, 2-phenylpyridine, and 2-(2,4-difluorophenyl)
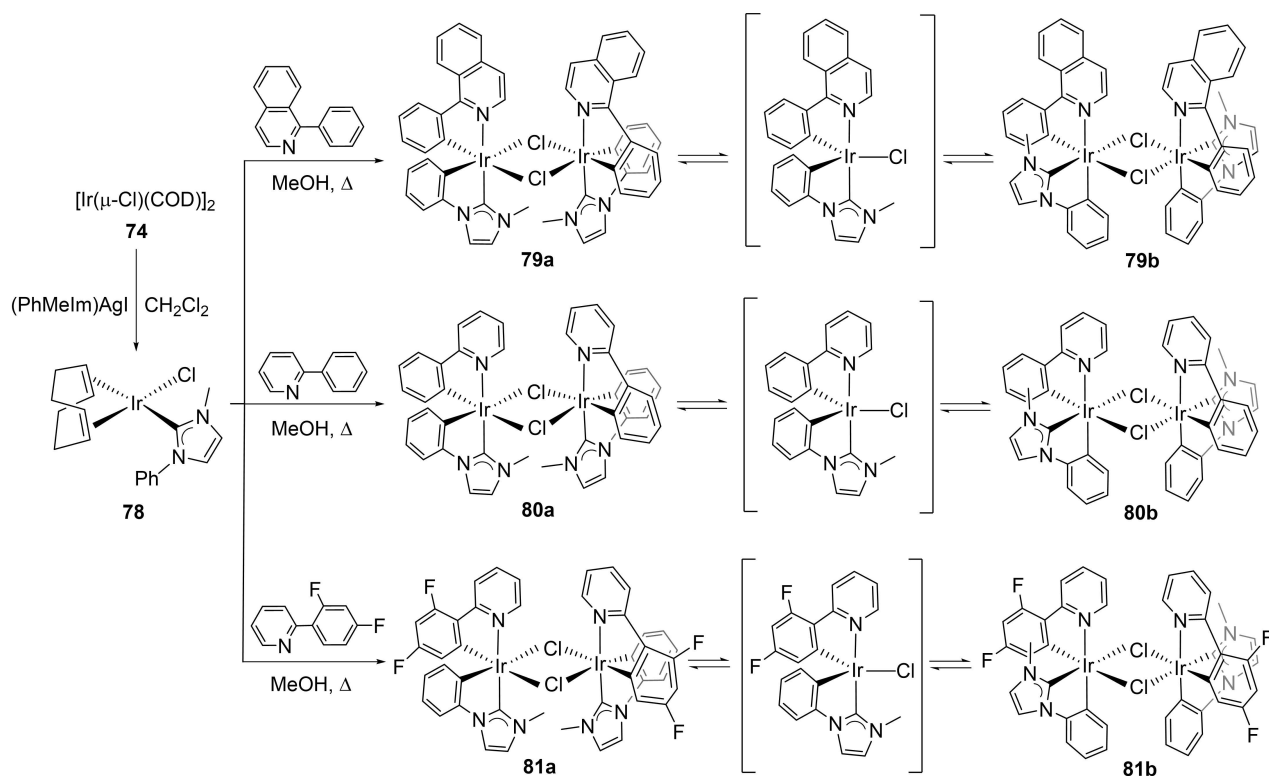
Scheme 21. Preparation of complexes **78–81**.

EurJIC
European Journal of Inorganic Chemistry

Minireviews
doi.org/10.1002/ejic.202100663

Chemistry Europe
European Chemical
Societies Publishing

pyridine, in methanol, under reflux (3–5 days) to afford the heteroleptic dimers **79–81**, as a result of the ortometalation of the coordinated phenyl-NHC ligand and the added aryl-heterocycle. In addition, the semi-hydrogenation of the coordinated diolefin, which is released as cyclooctene, takes place. The dimers were obtained as mixtures of the isomers **a** and **b**
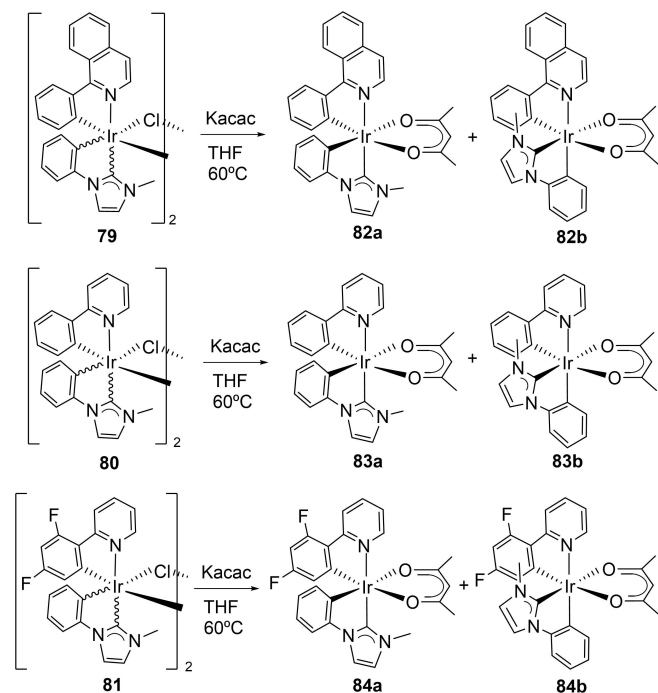
Scheme 22. Preparation of complexes **82–84**.
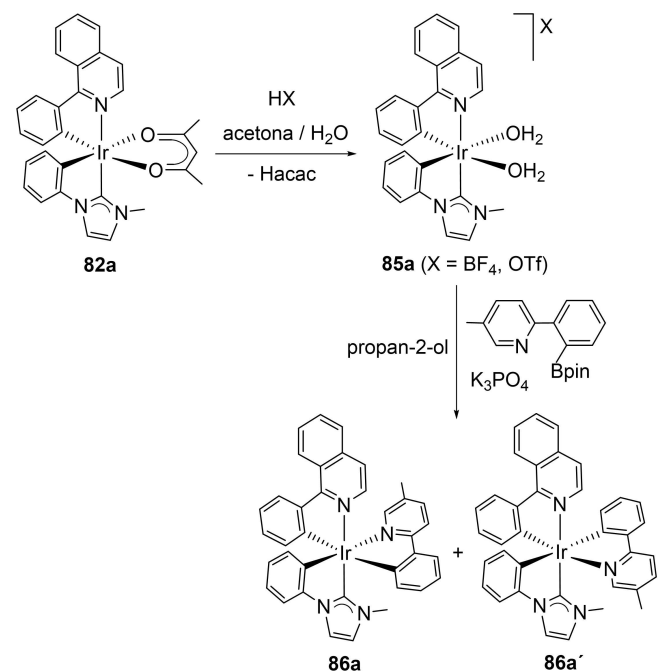
Scheme 23. Preparation of complexes **85–86**.

displayed in Scheme 21, in 81–70% yield. The structure of **79a** was confirmed by X-ray diffraction analysis.

The chloride bridges of complexes **79–81** were broken and further replaced by an acac ligand, through reaction with Kacac (Scheme 22). The respective acac complexes **82–84** were formed as mixtures of isomers **a** (NHC *trans* to N) and **b** (NHC *trans* to O) and obtained as pure solids in 10–60% yield after separation by column chromatography.

The substitution of the acac ligand of **82a** by an orthometalated 2-phenyl-5-methylpyridine group gives rise to an interesting [3b + 3b' + 3b''] emitter, containing two distinct orthometalated aryl-N-heterocycles and an orthometalated aryl-NHC. The procedure involves a base-assisted transmetalation from the boronated aromatic proligand to a *cis*-bis(aquo) intermediate (Scheme 23). Treatment 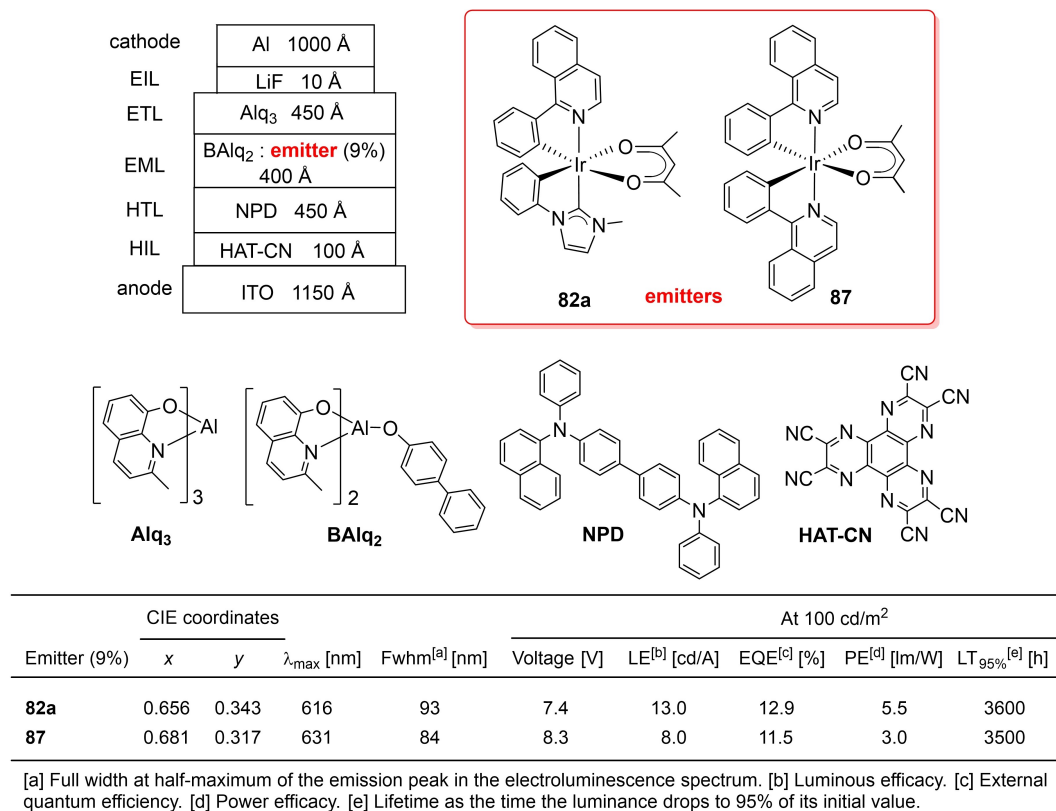of 3/1 acetone/water solutions of **82a** with excess of HBF_4 or HOTf (7 equiv) causes the protonation of the acac group and its replacement by two water molecules, to afford the water-solvato salts **85a**. In the presence of K_3PO_4, the borane 2-(2-pinacolborylphenyl)-5-methylpyridine transmetalates the *N,C*-ligand to the cation of the salts. The reaction leads to a mixture of two isomers, **86a** and **86a'**, which differs in the orientation of the cyclometalated 2-phenyl-5-methyl-pyridine. The molar ratio between them does not depend on the molar ratio between the boronated precursor and iridium, in a range of 1 to 15. Conversely, the amount of **86a** increases as the amount of K_3PO_4 increases; at K_3PO_4/iridium molar ratio > 40, this isomer is exclusively formed.

The phenylisoquinolinate derivatives **82a**, **82b**, and **86a** exhibit red emission, showing bands in the range of 580–652 nm, whereas compounds **83a**, **83b**, **84a**, and **84b** show green emission in the range of 465–532 nm (Table 1). The change in the orientation of the *C,C*-ligand causes a minimal modification in the emission color. The emissions of isomers **b** are slightly blue shifted with respect to those of the respective isomers **a**. As expected, the presence of two fluoride substituents in the orthometalated phenylpyridine of **84** also results in a moderate blue shift. The quantum yields in a PMMA film are in the range of 0.87 and 0.70 for the acac species **82–84**, whereas it drops to 0.34 for **86a**. The same is true in 2-MeTHF where the quantum yields for the acac complexes are between 0.93 and 0.56, while that of **86a** is 0.40.

The effect of the substitution of an orthometalated *C,N*-ligand by a *C,C*-aryl-NHC one has been analyzed by comparison of two similar OLED devices, one based on **82a** and the other one on **87**. The latter coordinates two cyclometalated 1-phenylisoquinoline groups and an acac ligand. Figure 4 shows the structure of the devices, the formulas of the compounds used in their construction, and their performance data. The substitution of the *C,N*-ligand by the *C,C*-moiety results in higher luminous and power efficacies. Thus, the comparison reveals that the performance of the OLED based on **82a** is higher or similar to that of the OLED based on **87**, demonstrating that [3b + 3b' + 3b''] complexes can be used as phosphorescent emitters in PHOLEDs despite their high propensity to ligand redistribution.

The use of pincer ligands decreases the number of structural isomers. With this principle in mind, the pincer

EurJIC
European Journal of Inorganic Chemistry

Minireviews
doi.org/10.1002/ejic.202100663

Chemistry Europe
European Chemical
Societies Publishing

Emitter (9%)	CIE coordinates		λ_{max} [nm]	Fwhm[a] [nm]	At 100 cd/m²				
	x	y			Voltage [V]	LE[b] [cd/A]	EQE[c] [%]	PE[d] [lm/W]	LT$_{95\%}$[e] [h]
82a	0.656	0.343	616	93	7.4	13.0	12.9	5.5	3600
87	0.681	0.317	631	84	8.3	8.0	11.5	3.0	3500

[a] Full width at half-maximum of the emission peak in the electroluminescence spectrum. [b] Luminous efficacy. [c] External quantum efficiency. [d] Power efficacy. [e] Lifetime as the time the luminance drops to 95% of its initial value.

Figure 4. Structure and performance data of the devices based on complexes **82a** and **87**. Abbreviations: HIL, hole-injector layer, HTL, hole-transporting layer, EML, emissive layer, ETL, electron-transporting layer, EIL, electron-injector layer.

coordination of 1,3-di(2-pyridyl)benzene (dpybH) was early attempted to build bis-tridentate iridium(III) emitters of the type [5t + 4t′].[47] In 2004, Williams et al. carried out the reaction between IrCl₃·3H₂O and dpybH under diverse conditions. Unfortunately, the activation of the C−H bond at the undesired 4-position of the benzene ring occurred, producing a bidentate ligand instead of the preferred pincer.[48] To gain a solution to this issue, 1,3-di(2-pyridyl)-4,6-dimethylbenzene (dpyMebH), with protected 4 and 6 positions, was prepared and subsequently reacted with IrCl₃·3H₂O in 2-ethoxyethanol. As expected, the reaction afforded the desired dimer [IrCl(μ-Cl)(dpyMeb)]₂ (**88**).[49] This compound is in fact a useful precursor to prepare [5t + 4t′] emitters, notwithstanding, we described in 2020 a synthetic procedure to obtain this type of emitters with the dpyb ligand as the 5t part of the structure.[50] The procedure was inspired by a previous work by Soro, Stoccoro, Manassero, et al. on palladium.[51] Initially the transmetalation of the dpyb from the mercury reagent Hg(dpyb)Cl to IrCl₃·3H₂O was tried to synthesize a dimer related to that of Williams with dpyMeb. Although the desired dimer **89** was obtained in high yield (70%; Scheme 24a), it is very insoluble in the usual solvents. At 80 °C, in dimethyl sulfoxide, the chloride bridges are broken and mononuclear species **90** is formed (23%); however, most of the dimer decomposes to a mixture of unidentified products. Against this background, complex **73**
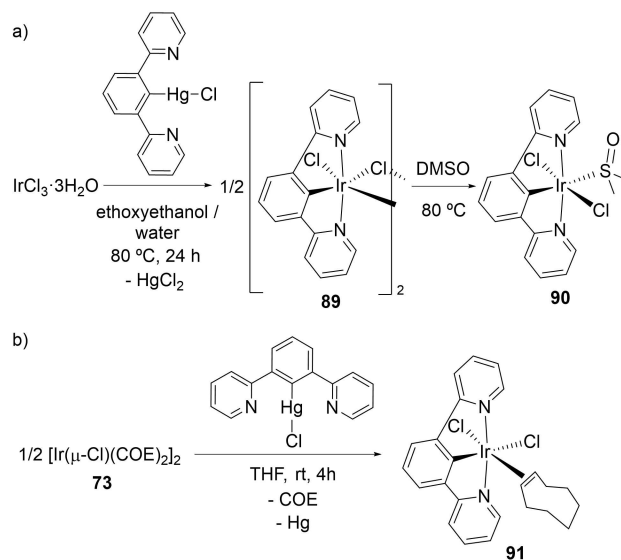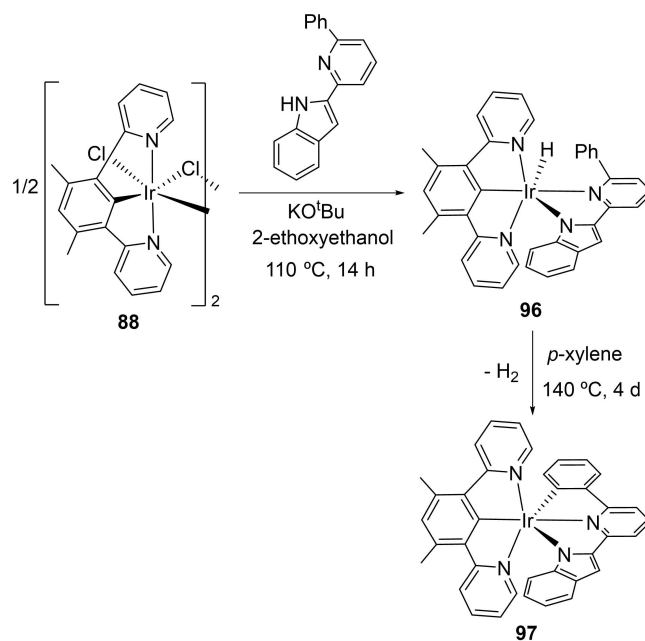

Scheme 24. Preparation of complexes **90** and **91**.

was employed as an alternative iridium precursor. The reaction of **73** with the mercury reagent, in tetrahydrofuran at room temperature, provided the iridium(III) derivative **91** in 51% yield (Scheme 24b). The process involves the transfer of the dpyb and chloride ligands from the mercury to the

EurJIC
European Journal of Inorganic Chemistry

Minireviews
doi.org/10.1002/ejic.202100663

Chemistry
Europe
European Chemical
Societies Publishing

iridium center, which is attached by the oxidation from iridium(I) to iridium(III) and the reduction from mercury(II) to mercury(0).[50] Complex **91** is a useful precursor to synthesize [5t + 4t'] emitters, in contrast to **89** and **90**. Its treatment with 2-(1H-imidazol-2-yl)-6-phenylpyridine and 2-(1H-benzimidazol-2-yl)-6-phenylpyridine, in the presence of Na$_2$CO$_3$, at 135 °C, for 3 days afforded **92** and **93**, respectively (Scheme 25a). The dpyMeb counterparts **94** and **95** were similarly prepared starting from the Williams's dimer **88** (Scheme 25b).

Complexes **92**–**95** display green emission (490–550 nm) in a doped PMMA film at 5 wt% and in 2-MeTHF (Table 1). The introduction of methyl groups at 3- and 5-position of the aryl group of the dipyridine-5t ligand or the substitution of the imidazole moiety by benzimidazole in the 4t' pincer does not affect the emission wavelength, which is in agreement with comparable HOMO–LUMO energy gaps for the four compounds (3.49–3.61 eV). On the other hand, complexes **94** and **95** bearing the methyl-substituted dpyMeb ligand exhibit higher quantum yields (between 0.50 and 0.70) than **92** and **93** (about 0.40), whereas the replacement of imidazole by benzimidazole in the 4 t' pincer has little or no effect on the phosphorescence efficiency of the emitters.

The effect of the uncoordinated N-atom of the 4t' ligand on the emissive features of **95** was studied by changing the benzimidazole fragment by an indole group. The synthesis of the emitter with the indole unit, **97**, was more complicated than that of **95**, requiring two steps and a strong base such as K^{t}BuO (Scheme 26). In the first step, the reaction of **88** with 2-(6-phenylpyridine-2-yl)-1H-indole and excess of the base (2.5 equiv), in 2-ethoxyethanol, at 110 °C for 14 h gave the monohydride intermediate **96**. In the second step, the heating of **96** in p-xylene, at 140 °C, for 4 days caused the ortho-CH bond activation of the phenyl substituent of the N,N-bidentate ligand and the relief a dihydrogen molecule, to give the desired emitter **97** in accordance with the known ability of platinum

Scheme 26. Preparation of complexes **96** and **97**.

group metal hydride complexes to promote the intramolecular activation of aryl-C–H bonds.[24] This complex exhibits greenish-yellow emission (547–624 nm) (Table 1). The presence of an indole instead of a benzimidazole in the 4t' ligand destabilizes the HOMO. As a consequence, the HOMO–LUMO energy gap decreases to 3.30 eV, which produces a red-shift of the emission. In addition, a decrease of the quantum yield until 0.20–0.30 is also noted.[50]

The heterocyclic substituent of the pyridine in the 4t' ligand of complexes **94**, **95**, and **97** has also been replaced with carbazolyl and phenoxy groups, with the aim of analyzing the
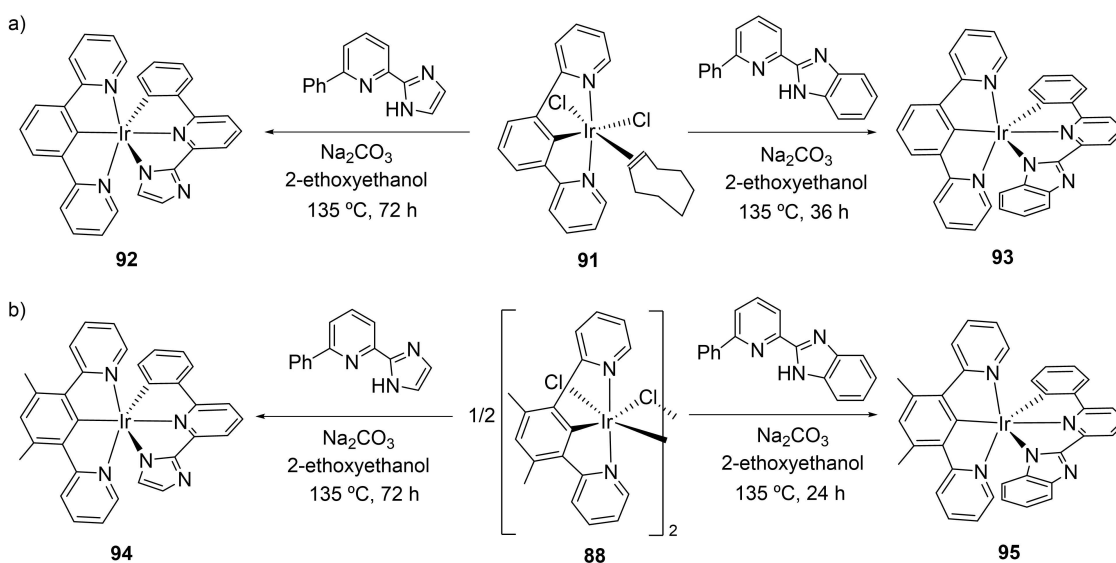
Scheme 25. Preparation of complexes **92**–**95**.

EurJIC
European Journal of Inorganic Chemistry

Minireviews
doi.org/10.1002/ejic.202100663

Chemistry Europe
European Chemical
Societies Publishing

impact of the formation of a six-membered metallaring on the photophysical properties of this class of emitters.[52] In this context, it should be further mentioned that carbazole derivatives are commonly used as host materials in PHOLEDs, due to their good hole-transporting capacity and high triplet energy.[53]

Complex **88** reacts with molten 9-(6-phenylpyridin-2-yl)-9*H*-carbazole and 2-phenoxy-6-phenylpyridine, in the presence of a silver salt (AgOTf), to give **98** and **99** (Scheme 27). The X-ray diffraction structures reveal that the carbazole of **98** and phenoxide of **99** coordinate to the iridium center through an η^1-arene π bond. The reaction of both intermediates with KO^{t}Bu gives rise to the respective [5t + 4t′] derivatives **100** and **101**, as a result of the deprotonation of the coordinated carbon atom of the η^1-arene group.

Complexes **100** and **101** are green emissive, displaying bands centered between 515 and 555 nm (Table 1). The quantum yields, in doped PMMA films (5 wt%), are 0.73 for **100** and 0.87 for **101**.[52] Emitter **101** is also an efficient photocatalyst for the synthesis of 3,3'-bioxindoles by dimerization of 3-bromooxindoles (Scheme 28).[54]

The 5t ligand of complexes **94** and **95** has been replaced with 5-*tert*-butyl-1,3-bis(3-isopropylimidazolylidene)phenyl. Because a dimer similar to **88** with this NHC ligand was not known, the first challenge was to obtain it. The strategy for its synthesis involved the used of [Ir(μ–OMe)(η^4–COD)]$_2$ (**102**) as starting material, since it bears a methoxide ligand able of carrying out the direct metalation of imidazolium salts. Treatment of **102** with a stoichiometric amount of the iodide salt of 5-tert-butyl-1,3-bis(3-isopropylimidazolium)benzene and an excess of KI, in 2-ethoxyethanol, at 120 °C for 18 h led to the iodide-bridged dimer **103**, which was isolated in 47% yield (Scheme 29). Complex **103** is very insoluble in the usual solvents (chlorinated solvents, acetone, alcohols, diethyl ether, and hydrocarbons). Nevertheless, the iodide bridges can be broken in acetonitrile, under reflux, to afford the mononuclear

Scheme 28. Synthesis of 3,3'-bioxindoles using **101** as photocatalyst.
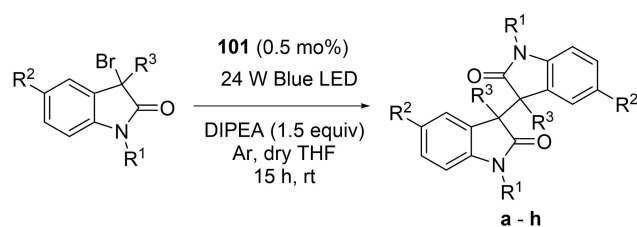
R^1	R^2	R^3	Product	Isolated yield
Me	H	Me	**a** (*R**,*R**):*meso* 1:1	72%
Me	OMe	Me	**b** (*R**,*R**):*meso* 1.2:1	51%
Benzyl	H	Me	**c** (*R**,*R**):*meso* 1.2:1	47%
Benzyl	OMe	Me	**d** (*R**,*R**):*meso* 1:1	30%
Me	H	Allyl	**e** (*R**,*R**):*meso* 1.2:1	70%
Me	OMe	Allyl	**f** (*R**,*R**):*meso* 1:1	25%
Benzyl	H	Allyl	**g** (*R**,*R**):*meso* 1:1	13%
Benzyl	OMe	Allyl	**h** (*R**,*R**):*meso* 1:1	20%

solvato complex **104**. Its X-ray structure reveals that, as expected, the *C,C',C*-ligand acts as a pincer with a NHC–Ir–NHC angle of approximately 155°.[55]

Dimer **103** reacts with 2-(1*H*-imidazol-2-yl)-6-phenylpyridine and 2-(1*H*-benzimidazol-2-yl)-6-phenylpyridine, in the presence of Na$_2$CO$_3$, under conditions similar to those employed to obtain **94** and **95**. The reactions give the NHC-counterparts **105** and **106** (Scheme 30). These compounds are green (482–567 nm) and yellowish green (506–590 nm) phosphorescent emitters (Table 1). The quantum yield of **105** (0.73) is significantly higher than that of **106** (0.49) in a doped PMMA film (5 wt%). However, in 2-MeTHF solution both emitters exhibit similar efficiency ($\approx$0.60).
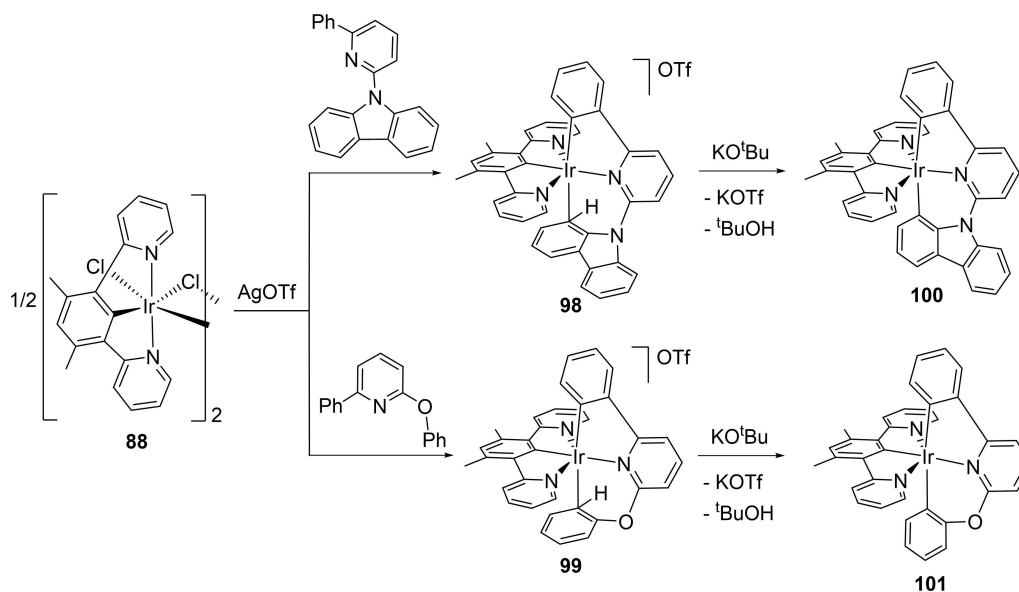
Scheme 27. Preparation of complexes **98**–**101**.

EurJIC
European Journal of Inorganic Chemistry

Minireviews
doi.org/10.1002/ejic.202100663

Chemistry Europe
European Chemical
Societies Publishing
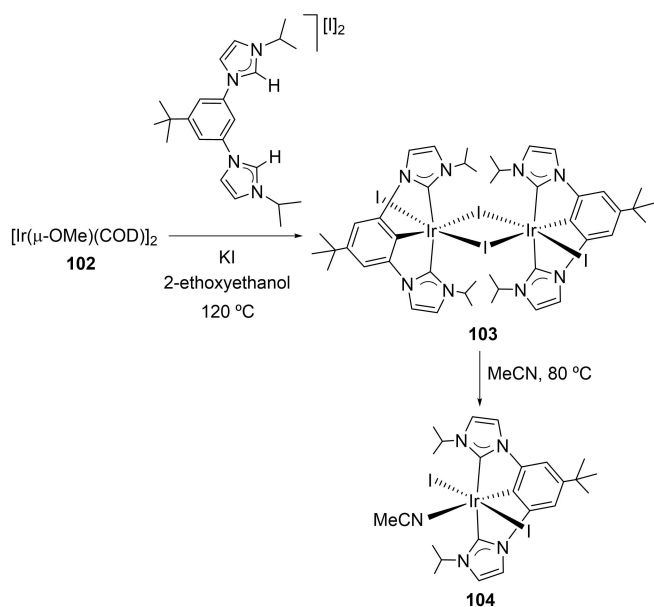
Scheme 29. Preparation of complexes **103** and **104**.
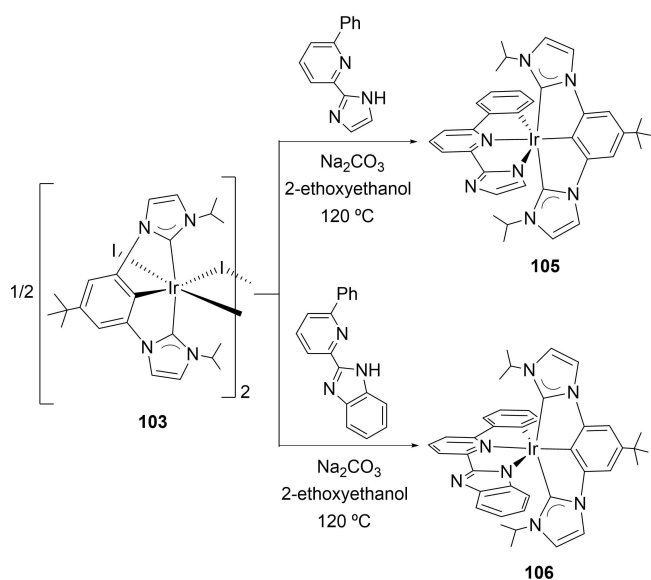
Scheme 30. Preparation of complexes **105** and **106**.

A PHOLED device containing complex **106** as emitter was compared with a parallel device based on *fac*-Ir(ppy)₃ (**107**; Hppy = 2-phenylpyridine), which is one of the most successful green phosphorescent emitters in the area of OLED display technology, with the aim of evaluating this type of [5t + 4t′] complexes as phosphorescent emitters. The schematic structure of the device, including the chemical structures of the device materials, and performance data are given in Figure 5. Although complex **106** proves its usefulness for manufacturing OLED devices, the overall performance of its device is poorer than that of **107**.

Dimer **102** is also a suitable precursor to obtain an interesting [Ir(*u*-Cl)(6tt)]₂ dimer, bearing two cyclometalated phenylimidazolylidene units connected by a butylene chain, which allowed us an easy entry to blue-green [6tt + 3b] emitters displaying quantum yields close to unity.[56] The use of the pentahydride **51** as starting material is not recommended in this case, since it gives a dinuclear complex with a bridging bis (NHC)-ligand.[57] Treatment of suspensions of **102** with 1,1′-diphenyl-3,3-butylenediimidazolium diiodide and NaO^tBu in 2-methoxyethanol, at 130 °C, for 6 h gives the iodide-bridged dimer **108** in 65 % yield (Scheme 31). Abstraction of the iodide bridges with AgOTf, in acetone/dichloromethane, followed by the addition of a KOH methanol solution leads to the methoxide-hydroxide-bridged dinuclear compound **109**. Thi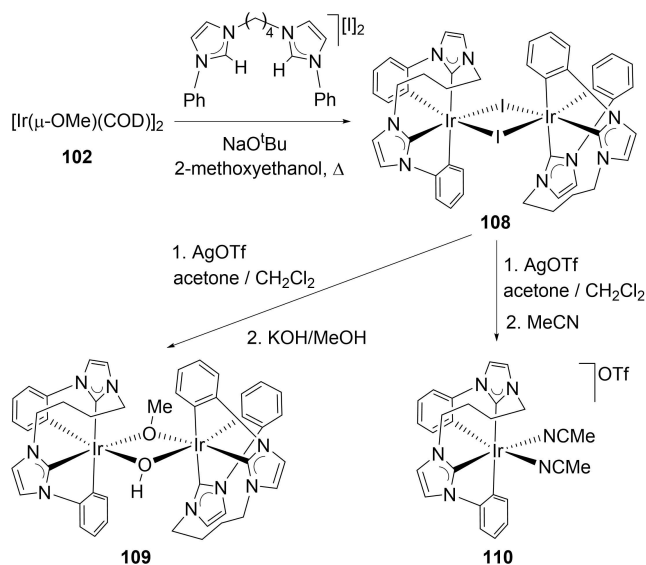s compound was isolated in 47 % yield and characterized by X-ray diffraction analysis. Its structure revealed that the two imidazolylidene moieties are mutually *cis*-oriented,[56] in contrast to that observed in the [Ir(*u*-Cl)(3b)₂]₂ dimers, containing two free cyclometalated Aryl-NHC ligands, where the NHC groups are mutually *trans*-disposed.[58] The abstraction of the halide ligands of **108** with AgOTf, in acetone/dichloromethane, affords a complex mixture of solvato compounds. In acetonitrile, this mixture affords the mononuclear bis(acetonitrile) derivative **110**, as a white solid in 71 % yield. Cation of **110** is the true precursor of the blue-green emitters.

Complex **110** heterolytically activates the *ortho*-CH bond of the phenyl substituent of a variety of 2-phenylpyridines, using (piperidinomethyl)polystyrene as an external base. The reactions were carried out in fluorobenzene, under reflux, and tolerated substituents at both the phenyl and pyridyl groups (Scheme 32). Thus, 2-phenylpyridine, 2-(2,4-difluorophenyl) pyridine, 2-(*p*-tolyl)pyridine, and 5-methyl-2-phenylpyridine afforded the respective derivatives **111**–**114** as pure solids, in high yields (80–95 %), without extra purification.[56]

Scheme 31. Preparation of complexes **108**–**110**.

EurJIC
European Journal of Inorganic Chemistry

Minireviews
doi.org/10.1002/ejic.202100663

Chemistry Europe
European Chemical Societies Publishing

| Emitter (10%)	CIE coordinates		λ_{max} [nm]	Fwhm[a] [nm]	max EQE[b] [%]	At 1000 cd/m^2			
	x	y				Voltage [V]	LE[c] [cd/A]	EQE [%]	PE[d] [lm/W]
106	0.458	0.530	552	85	12.0	8.0	28.8	9.3	11.3
107	0.304	0.630	518	68	14.3	5.8	46.9	13.1	25.5

[a] Full width at half-maximum of the emission peak in the electroluminescence spectrum. [b] External quantum efficiency. [c] Luminous efficacy. [d] Power efficacy.

Figure 5. Structure and performance data of the devices based on complexes **106** and **107**. Abbreviations: HIL, hole-injector layer, HTL, hole-transporting layer, EML, emissive layer, HBL, hole-blocking layer, ETL, electron-transporting layer, EIL, electron-injector layer.
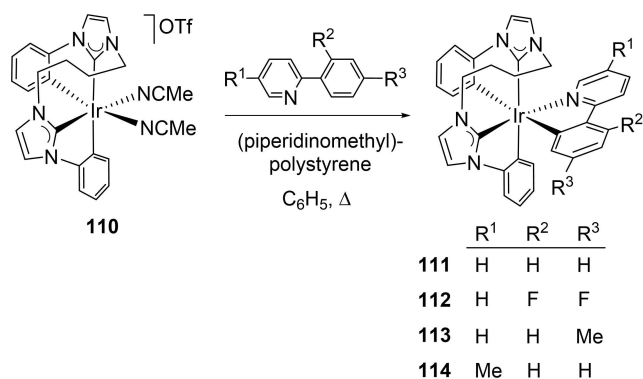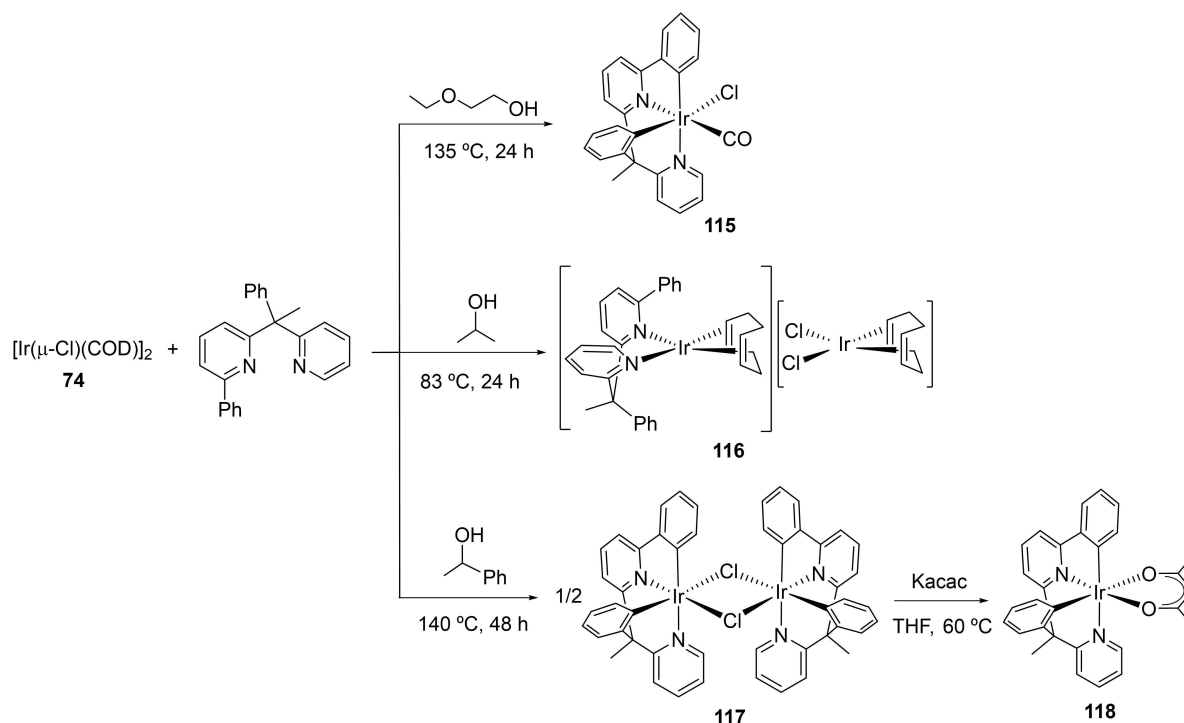

Scheme 32. Preparation of complexes **111–114**.

Complexes **111–114** display blue-green phosphorescent emission (455–510 nm) with lifetimes between 1.3 and 4.8 µs (Table 1). The quantum yields of the four compounds in PMMA films are close to unity (0.87–0.96), whereas they are ~1 for **111**, **113**, and **114** and 0.73 for **112** in 2-MeTHF at 298 K.

An interesting approach to the solution of the issues associated to the preparation of heteroleptic [3b+3b'+3b''] emitters is to link two different bidentate ligands, 3b and 3b', to generate an heteroleptic 6e-donor tetradentate ligand, 6tt'. In this manner, without undermining the heteroleptic character of the emitter, the ligand distribution possibilities are reduced. This allows higher reaction yields and enables the chromatographic separation. Moreover, a better structural control should be achieved as a consequence of the higher rigidity of the system, which results in a decrease in the number of viable stereoisomers. In the search for confirming the goodness of this idea, 2-phenyl-6-(1-phenyl-1-(pyridin-2-yl)ethyl)pyridine has been recently prepared and its coordination to iridium investigated. This molecule, which is formed by attached 2-phenylpyridine and 2-benzylpyridine moieties, reacts with the dimer **74** in alcohols as solvent. The products obtained depend upon the alcohol nature and its refluxing temperature. Primary alcohols produce the carbonylation of the iridium center, while secondary ones must have a high boiling temperature to promote the *ortho*-C–H bond activation of the phenyl rings of the proligand.[59] Thus, complexes **115**, **116**, and **117** were obtained in 2-ethoxyethanol, propan-2-ol, and 1-phenylethanol, respectively. The reaction of complex **117** with Kacac affords the acac derivative **118** (Scheme 33). The latter can be seen as a *pseudo*-tris(heteroleptic) compound of iridium(III), whose coordination sphere is formed by three different bidentate moieties, an orthometalated 2-phenylpyridine, an orthometalated 2-benzylpyridine, and an acac. The X-ray structures of **115** and **118** disclose that the ligand design enforces a mutually *cis* disposition of the pyridine units, which is in contrast to that usually found for hetreoleptic iridium(III)

EurJIC
European Journal of Inorganic Chemistry

Minireviews
doi.org/10.1002/ejic.202100663

Chemistry Europe
European Chemical
Societies Publishing

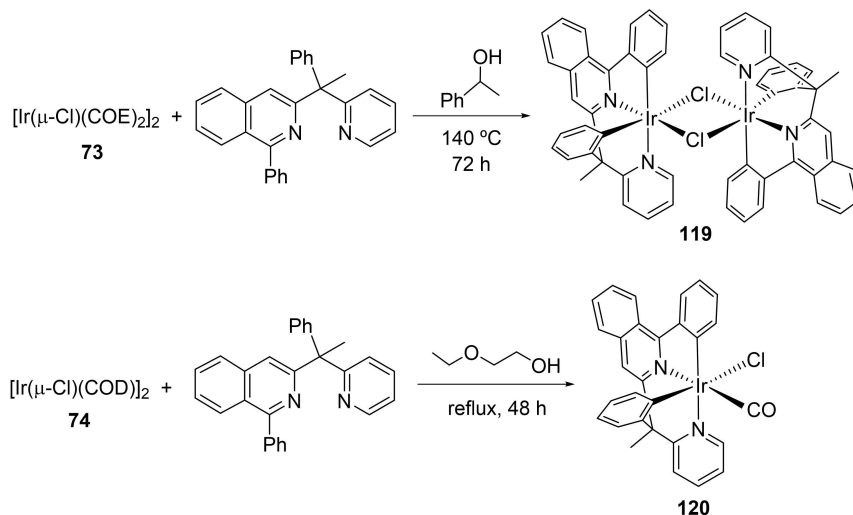**Scheme 33.** Preparation of complexes 115–118.

complexes containing two orthometalated 2-phenylpyridines. Other two ligands of this class have been used with a similar purpose. The 2,2′-(1-(6-(3-trifluoromethyl-1H-pyrazol-5-yl)pyridin-2-yl)ethane-1,1-diyl)dipyridine molecules afford monoanionic N,N′,N′′,N′′-tetradentate ligands (7tt′), which stabilize sky blue [7tt′ + 2b] emitters,[60] whereas the replacement of one peripheral pyridine with a phenyl group leads to 2-(3-trifluoromethyl-1H-pyrazol-5-yl)-6-(1-phenyl-1-(pyridyn-2-yl)ethyl)pyridine, which forms a dianionic N,N′,C,N′′-tetradentate ligand 6tt′. This anion uses the free N-atom of the pyrazolate group to afford a green binuclear emitter.[61]

Complexes 115 and 118 are phosphorescent emitters, as expected (Table 1). The former exhibits blue-green emission (468–541 nm), whereas the latter displays emission in the green region (527–562 nm). This difference is in agreement with the DFT-calculated HOMO–LUMO gap, smaller for 118 (3.71 eV) than for 115 (3.98 eV). The lifetimes are alike for both emitters (1.1–4.5 μs). The quantum yield of 115 in PMMA is considerably higher than in 2-MeTHF (0.87 vs 0.54); consequently, the ratio between the radiative and nonradiative rate constants is >5 times greater in the film than in the solution. Contrary to 115, compound 118 shows similar photoluminescence quantum yields in both media (0.71 vs 0.66) and also similar ratios between the rate constants.[59]
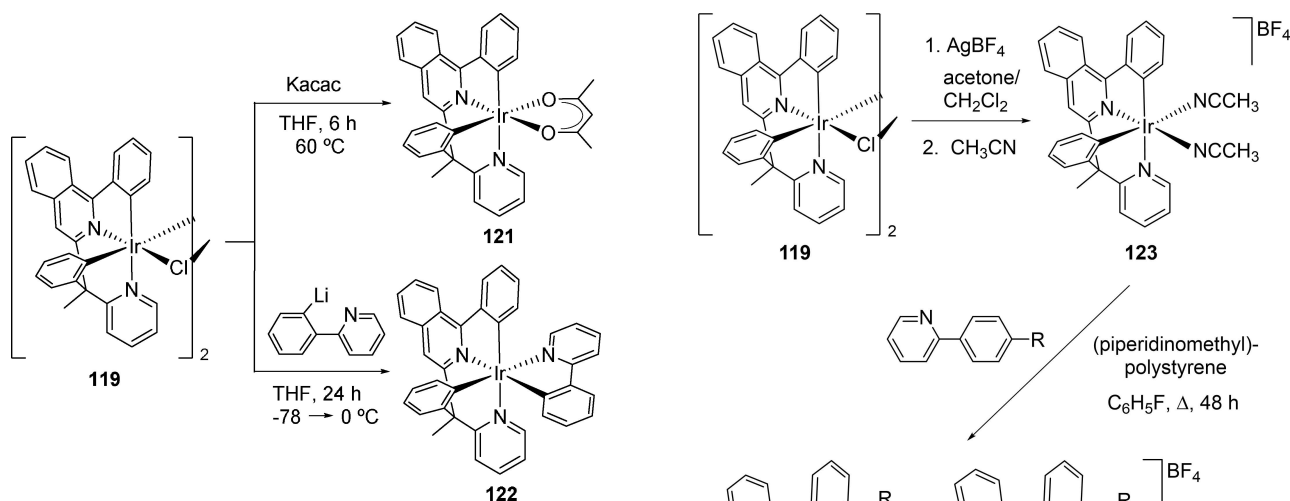
The phenylpyridine group of 2-phenyl-6-(1-phenyl-1-(pyridin-2-yl)ethyl)pyridine has been replaced with a phenylisoquinoline unit in the search for red emitters with structural rigidity similar to that of 118.[62] The resulting organic molecule, 1-phenyl-3-(1-phenyl-1-(pyridine-2-yl)ethyl)isoquinoline, reacts with the dimers 73 and 74 in 2-ethoxyethanol and 1-phenyl-

ethanol to afford the dimer 119 and the carbonyl derivative 120, respectively, which were isolated in 82% and 66% yields. The X-ray structure of 120 revealed that, in these compounds, the N-heterocyclic rings are mutually cis-disposed and the phenyl rings are also cis-arranged, as in complexes 115, 117, and 118. (Scheme 34).

Dimer 119 reacts with Kacac and Li[py-2-C$_6$H$_4$]. The reactions lead to the acac-derivative 121, an isoquinolyl counterpart of 118, and the tris-heterocyclic species 122 with a fac-disposition of the nitrogen containing rings. Both compounds retain the disposition of the tetradentate ligand on the metal coordination sphere (Scheme 35). Such a disposition is also present in the acetonitrile-solvato 123 (Scheme 36). In contrast to the dimer 119, the mononuclear solvento complex 123 is the starting point to interesting pyridyl-benzyl position exchanges. Treatment of fluorobenzene solutions of 123 with 2-phenylpyridine and (piperidinomethyl)polystyrene under reflux leads to a mixture of 124, a mer-isomer of 122 retaining the tetradentate ligand disposition, and the salt 125 bearing the phenyl ring of the benzyl group η^2-coordinated to metal center of the cation. The formation of this cation implies a hydrogen-transfer reaction at the iridium coordination sphere from the phenyl substituent of the incoming pyridine to the aryl unit of the benzyl moiety of the tetradentate ligand. Furthermore, the anticipated position exchange between the pyridyl and phenyl rings of the benzylpyridine group takes place. Under the same conditions as those employed with 2-phenyl-pyridine, the reaction of 123 with 2-(p-tolyl)pyridine gives a

EurJIC
European Journal of Inorganic Chemistry

Minireviews
doi.org/10.1002/ejic.202100663

Chemistry Europe
European Chemical
Societies Publishing

Scheme 34. Preparation of complexes **119** and **120**.

Scheme 35. Preparation of complexes **121** and **122**.

Scheme 36. Preparation of complexes **124**–**127**.

mixture of **126** and **127**. In the absence of base, in refluxing 2-propanol, the salts **125** and **127** are selectively formed.

The η^2-coordination enhances the acidity of the *ortho*-CH bond. As a consequence of the acidity increase, the addition of KO^{t}Bu to tetrahydrofuran solutions of the salts **125** and **127** produces the deprotonation of the coordinated bond and the formation of the respective *mer*-isomers **128** and **129**, bearing the phenyl groups of the tetradentate ligand disposed mutually *trans* and the pyridyl ring of the bidentate ligand situated *trans* to the isoquinolyl group (Scheme 37).

Complexes **120**–**122** and **124**–**129** are red emitters (Table 1) with emission in the range of 601–732 nm, which exhibit short lifetimes (0.7–4.6 µs) and quantum yields in PMMA film at 5 wt % and 2-MeTHF between 0.08 and 0.58. The acac-derivative **121**, with a noticeable quantum yield of about 0.60, was used as a dopant for a red PhOLED and the device was compared with that of **87**. Figure 6 maps the devices structure, the

Scheme 37. Preparation of complexes **128** and **129**.

EurJIC
European Journal of Inorganic Chemistry

Minireviews
doi.org/10.1002/ejic.202100663

Chemistry Europe
European Chemical
Societies Publishing

Emitter (9%)	CIE coordinates				At 10 mA/cm²				
	x	y	λ_{max} [nm]	Fwhm[a] [nm]	Voltage [V]	LE[b] [cd/A]	EQE[c] [%]	PE[d] [lm/W]	LT$_{95\%}$[e] [h]
121	0.556	0.390	672	118	8.2	0.9	3.4	0.3	17724
87	0.674	0.323	630	78	8.4	8.5	12.4	3.2	7522

[a] Full width at half-maximum of the emission peak in the electroluminescence spectrum. [b] Luminous efficacy. [c] External quantum efficiency. [d] Power efficacy. [e] Lifetime as the time the luminance drops to 95% of its initial value.

Figure 6. Structure and performance data of the devices based on complexes **82 a** and **87**. Abbreviations: HIL, hole-injector layer, HTL, hole-transporting layer, EML, emissive layer, ETL, electron-transporting layer, EIL, electron-injector layer.

chemical components, and the main performance data. Although complex **121** proves to have applicability to the fabrication of OLED devices; its features are in general poorer than those of **87**.

4. Summary and Outlook

The improvement of the features of phosphorescent emitters of osmium, iridium, and platinum has been traditionally based on the design of organic chromophores, which coordinate the desired 5d metal by means of a limited number of standard methods. Previous pages show a different point of view. Without wishing in any way to detract from the importance of organic synthesis, the progress of the field is based on the application and development of new procedures of organometallic synthesis and the search for alternative starting complexes. As a result of this strategy, there has been a significant enhancement in the synthesis of osmium(IV), osmium(II), and iridium(III) emitters since 2012, which has allowed the discovery of novel classes of emitters of these central ions, being particularly noticeable the advances in osmium(IV). The ongoing progress is mainly a consequence of the ability of the alternative starting compounds used to promote the activation of σ-bonds of the chromophores, which certainly facilitates their entry into the metal coordination sphere. The use of more rational synthetic strategies involving

more organometallic chemistry is other feature to be highlighted.

The relevance of the osmium-hexahydride $OsH_6(P^iPr_3)_2$ should be pointed out, since it has allowed the preparation of most of the currently known osmium(IV) emitters, which in some cases reach quantum yields of about 0.60 for orange-red emissions, although it is certainly necessary much more effort to achieve the full maturity of this class of emitters. Furthermore, this starting complex has proven to be an excellent entry to homoleptic and heteroleptic osmium(II) emitters, including the blue emitter **37** which has demonstrated its usefulness in the manufacture of OLED devices with a device efficiency comparable to that of the state-of-the art iridium(III)-based devices. In line with $OsH_6(P^iPr_3)_2$, the iridium-pentahydride $IrH_5(P^iPr_3)_2$ is other manifestation of the usefulness of polyhydride complexes as synthetic precursors to the preparation of emitters, in this case in the iridium chemistry. The ability of the polyhydrides of platinum group metals to activate C−H bonds has undoubtedly been the determining factor in these successes.

The choice of the starting compound should be done taking into account the function of its ligands during the synthesis, since they are not just mere spectators, which fine-tune the electron density of the central ion and its surrounding space, but can also cooperate in the synthesis of the emitter. Three different functions have been clearly identified in the revised procedures: they can direct the selectivity of competitive

EurJIC
European Journal of Inorganic Chemistry

Minireviews
doi.org/10.1002/ejic.202100663

Chemistry
Europe
European Chemical
Societies Publishing

ruptures of σ-bonds of the chromophores without having direct participation in the activation; on the contrary, they can directly participate in the generation of a ligand, on the metal coordination sphere, being a part of the new coordinated group; and they can act as an internal base in σ-bond heterolytic activation reactions.

The reaction conditions are other aspect to pay special attention to. Many reactions are performed in alcohols or oxygenated organic solvents and their choice is a crucial step in the planning of the synthesis. Not only because they decide the solubility of reagents and products and the maximum temperature, but also because they may be sources of the carbonyl ligand, in particular when high temperatures are necessary.

In summary, novel and creative organometallic synthesis is necessary to design and develop new and better phosphorescent emitters.

Acknowledgements

Conflict of Interest

The authors declare no conflict of interest.

[1] M. A. Baldo, D. F. O'Brien, Y. You, A. Shoustikov, S. Sibley, M. E. Thompson, S. R. Forrest, *Nature* **1998**, *395*, 151–154.

[2] a) P.-T. Chou, Y. Chi, M.-W. Chung, C.-C. Lin, *Coord. Chem. Rev.* **2011**, *255*, 2653–2665; b) B. J. Powell, *Coord. Chem. Rev.* **2015**, *295*, 46–79.

[3] H. Yersin, A. F. Rausch, R. Czerwieniec, T. Hofbeck, T. Fischer, *Coord. Chem. Rev.* **2011**, *255*, 2622–2652.

[4] a) R. D. Costa, E. Ortí, H. J. Bolink, F. Monti, G. Accorsi, N. Armaroli, *Angew. Chem. Int. Ed.* **2012**, *51*, 8178–8211; *Angew. Chem.* **2012**, *124*, 8300–8334; b) T. Hu, L. He, L. Duan, Y. Qiu, *J. Mater. Chem.* **2012**, *22*, 4206–4215; c) K. J. Suhr, L. D. Bastatas, Y. Shen, L. A. Mitchell, G. A. Frazier, D. W. Taylor, J. D. Slinker, B. J. Holliday, *Dalton Trans.* **2016**, *45*, 17807–17823; d) A. F. Henwood, E. Zysman-Colman, *Chem. Commun.* **2017**, *53*, 807–826.

[5] a) E. Baranoff, J.-H. Yum, M. Graetzel, Md. K. Nazeeruddin, *J. Organomet. Chem.* **2009**, *694*, 2661–2670; b) L. Xiao, Z. Chen, B. Qu, J. Luo, S. Kong, Q. Gong, J. Kido, *Adv. Mater.* **2011**, *23*, 926–952; c) C. Fan, C. Yang, *Chem. Soc. Rev.* **2014**, *43*, 6439–6469; d) X. Yang, G. Zhou, W.-Y. Wong, *Chem. Soc. Rev.* **2015**, *44*, 8484–8575; e) J.-H. Jou, S. Kumar, A. Agrawal, T.-H. Li, S. Sahoo, *J. Mater. Chem. C* **2015**, *3*, 2974–3002; f) S. Huo, J. Carroll, D. A. K. Vezzu, *Asian J. Org. Chem.* **2015**, 4, 1210–1245; g) C.-W. Lu, Y. Wang, Y. Chi, *Chem. Eur. J.* **2016**, *22*, 17892–17908.

[6] a) P.-T. Chou, Y. Chi, *Eur. J. Inorg. Chem.* **2006**, 3319–3332; b) Y. Chi, P.-T. Chou, *Chem. Soc. Rev.* **2007**, *36*, 1421–1431; c) Y. Chi, P.-T. Chou, *Chem. Soc. Rev.* **2010**, *39*, 638–655; d) Y. Chi, B. Tong, P.-T. Chou, *Coord. Chem. Rev.* **2014**, *281*, 1–25; e) Y. Zhang, Y. Wang, J. Song, J. Qu, B. Li, W. Zhu, W.-Y. Wong, *Adv. Opt. Mater.* **2018**, *6*, 1800466.

[7] a) A. B. Tamayo, B. D. Alleyne, P. I. Djurovich, S. Lamansky, I. Tsyba, N. N. Ho, R. Bau, M. E. Thompson, *J. Am. Chem. Soc.* **2003**, *125*, 7377–7387; b) J. Li, P. I. Djurovich, B. D. Alleyne, M. Yousufuddin, N. N. Ho, J. C. Thomas, J. C. Peters, R. Bau, M. E. Thompson, *Inorg. Chem.* **2005**, *44*,

1713–1727; c) K. Dedeian, J. Shi, N. Shepherd, E. Forsythe, D. C. Morton, *Inorg. Chem.* **2005**, *44*, 4445–4447; d) R. Ragni, E. A. Plummer, K. Brunner, J. W. Hofstraat, F. Babudri, G. M. Farinola, F. Naso, L. De Cola, *J. Mater. Chem.* **2006**, *16*, 1161–1170; e) I. Avilov, P. Minoofar, J. Cornil, L. De Cola, *J. Am. Chem. Soc.* **2007**, *129*, 8247–8258; f) H. Benjamin, Y. Zheng, V. N. Kozhevnikov, J. S. Siddle, L. J. O'Driscoll, M. A. Fox, A. S. Batsanov, G. C. Griffiths, F. B. Dias, A. P. Monkman, M. R. Bryce, *Dalton Trans.* **2020**, *49*, 2190–2208.

[8] a) Y.-J. Su, H.-L. Huang, C.-L. Li, C.-H. Chien, Y.-T. Tao, P.-T. Chou, S. Datta, R.-S. Liu, *Adv. Mater.* **2003**, *15*, 884–888; b) H. A. Bronstein, C. E. Finlayson, K. R. Kirov, R. H. Friend, C. K. Williams, *Organometallics* **2008**, *27*, 2980–2989; c) Z. Chen, H. Zhang, D. Wen, W. Wu, Q. Zeng, S. Chen, W.-Y. Wong, *Chem. Sci.* **2020**, *11*, 2342–2349; d) H. Zhang, H. Wang, K. Tanner, A. Schlachter, Z. Chen, P. D. Harvey, S. Chen, W.-Y. Wong, *Dalton Trans.* **2021**, *50*, 10629–10639; e) K. M. Kuznetsov, I. S. Kritchenkov, J. R. Shakirova, V. V. Gurzhiy, V. V. Pavlovskiy, V. V. Porsev, V. V. Sokolov, S. P. Tunik, *Eur. J. Inorg. Chem.* **2021**, 2163–2170.

[9] a) S.-W. Lai, Q. K.-W. Chan, N. Zhu, C.-M. Che, *Inorg. Chem.* **2007**, *46*, 11003–11016; b) T.-C. Lee, J.-Y. Hung, Y. Chi, Y.-M. Cheng, G.-H. Lee, P.-T. Chou, C.-C. Chen, C.-H. Chang, C.-C. Wu, *Adv. Funct. Mater.* **2009**, *19*, 2639–2647; c) J.-L. Chen, Y. Chi, K. Chen, Y.-M. Cheng, M.-W. Chung, Y.-C. Yu, G.-H. Lee, P.-T. Chou, C.-F. Shu, *Inorg. Chem.* **2010**, *49*, 823–832; d) C.-C. Hsu, C.-C. Lin, P.-T. Chou, C.-H. Lai, C.-W. Hsu, C.-H. Lin, Y. Chi, *J. Am. Chem. Soc.* **2012**, *134*, 7715–7724; e) S.-H. Chang, C.-F. Chang, J.-L. Liao, Y. Chi, D.-Y. Zhou, L.-S. Liao, T.-Y. Jiang, T.-P. Chou, E. Y. Li, G.-H. Lee, T.-Y. Kuo, P.-T. Chou, *Inorg. Chem.* **2013**, *52*, 5867–5875; f) J.-L. Liao, Y. Chi, Y.-D. Su, H.-X. Huang, C.-H. Chang, S.-H. Liu, G.-H. Lee, P.-T. Chou, *J. Mater. Chem. C* **2014**, *2*, 6269–6282; g) W.-K. Chu, S.-M. Yiu, C.-C. Ko, *Organometallics* **2014**, *33*, 6771–6777; h) J.-L. Liao, Y. Chi, S.-H. Liu, G.-H. Lee, P.-T. Chou, H.-X. Huang, Y.-D. Su, C.-H. Chang, J.-S. Lin, M.-R. Tseng, *Inorg. Chem.* **2014**, *53*, 9366–9374; i) J.-L. Liao, Y. Chi, C.-C. Yeh, H.-C. Kao, C.-H. Chang, M. A. Fox, P. J. Low, G.-H. Lee, *J. Mater. Chem. C* **2015**, *3*, 4910–4920; j) Y.-H. Li, X.-L. Liu, Z.-T. Yu, Z.-S. Li, S.-C. Yan, G.-H. Chen, Z.-G. Zou, *Dalton Trans.* **2016**, *45*, 12400–12408; k) Y. Yuan, J.-L. Liao, S.-F. Ni, A. K.-Y. Jen, C.-S. Lee, Y. Chi, *Adv. Funct. Mater.* **2020**, *30*, 1906738.

[10] a) C. Ulbricht, B. Beyer, C. Friebe, A. Winter, U. S. Schubert, *Adv. Mater.* **2009**, *21*, 4418–4441; b) Z. Liu, Z. Bian, C. Huang, *Top. Organomet. Chem.* **2010**, *28*, 113–142; c) Y. You, W. Nam, *Chem. Soc. Rev.* **2012**, *41*, 7061–7084; d) K. P. S. Zanoni, R. L. Coppo, R. C. Amaral, N. Y. M. Iha, *Dalton Trans.* **2015**, *44*, 14559–14573; e) I. Omae, *Coord. Chem. Rev.* **2016**, *310*, 154–169; f) Y. Im, S. Y. Byun, J. H. Kim, D. R. Lee, C. S. Oh, K. S. Yook, J. Y. Lee, *Adv. Funct. Mater.* **2017**, *27*, 1603007; g) T.-Y. Li, J. Wu, Z.-G. Wu, Y.-X. Zheng, J.-L. Zuo, Y. Pan, *Coord. Chem. Rev.* **2018**, *374*, 55–92; h) Y. Chi, S. F. Wang, P. Ganesan, *Chem. Rec.* **2019**, *19*, 1644–1666; i) S. Lee, W.-S. Han, *Inorg. Chem. Front.* **2020**, *7*, 2396–2422; j) A. Bonfiglio, M. Mauro, *Eur. J. Inorg. Chem.* **2020**, 3427–3442.

[11] a) J. Lalevée, M. Peter, F. Dumur, D. Gigmes, N. Blanchard, M.-A. Tehfe, F. Morlet-Savary, J. P. Fouassier, *Chem. Eur. J.* **2011**, *17*, 15027–15031; b) C. K. Prier, D. A. Rankic, D. W. C. MacMillan, *Chem. Rev.* **2013**, *113*, 5322–5363; c) D. M. Arias-Rotondo, J. K. McCusker *Chem. Soc. Rev.* **2016**, *45*, 5803–5820; d) M.-A. Tehfe, M. Lepeltier, F. Dumur, D. Gigmes, J.-P. Fouassier, J. Lalevée, *Macromol. Chem. Phys.* **2017**, *218*, 1700192; e) L. Marzo, S. K. Pagire, O. Reiser, B. König, *Angew. Chem. Int. Ed.* **2018**, *57*, 10034–10072; *Angew. Chem.* **2018**, *130*, 10188–10228; f) I. N. Mills, J. A. Porras, S. Bernhard, *Acc. Chem. Res.* **2018**, *51*, 352–364.

[12] a) S. Bettington, M. Tavasli, M. R. Bryce, A. S. Batsanov, A. L. Thompson, H. A. Al Attar, F. B. Diasb, A. P. Monkman, *J. Mater. Chem.* **2006**, *16*, 1046–1052; b) A. M'hamedi, A. S. Batsanov, M. A. Fox, M. R. Bryce, K. Abdullah, H. A. Al-Attar, A. P. Monkman, *J. Mater. Chem.* **2012**, *22*, 13529–13540; c) Y. Zheng, A. S. Batsanov, M. A. Fox, H. A. Al-Attar, K. Abdullah, V. Jankus, M. R. Bryce, A. P. Monkman, *Angew. Chem. Int. Ed.* **2014**, *53*, 11616–11619; *Angew. Chem.* **2014**, *126*, 11800–11803; d) J. Fernández-Cestau, N. Giménez, E. Lalinde, P. Montaño, M. T. Moreno, S. Sánchez, *Organometallics* **2015**, *34*, 1766–1778; e) M. Y. Wong, G. Xie, C. Tourbillon, M. Sandroni, D. B. Cordes, A. M. Z. Slawin, I. D. W. Samuel, E. Zysman-Colman, *Dalton Trans.* **2015**, *44*, 8419–8432; f) X. Yang, X. Xu, J.-S. Dang, G. Zhou, C.-L. Ho, W.-Y. Wong, *Inorg. Chem.* **2016**, *55*, 1720–1727; g) X. Yang, Z. Feng, J. Zhao, J.-S. Dang, B. Liu, K. Zhang, G. Zhou, *ACS Appl. Mater. Interfaces* **2016**, *8*, 33874–33887; h) D. G. Congrave, Y.-T. Hsu, A. S. Batsanov, A. Beeby, M. R. Bryce, *Organometallics* **2017**, *36*, 981–993; i) Y.-J. Cho, S.-Y. Kim, C. M. Choi, N. J. Kim, C. H. Kim, D. W. Cho, H.-J. Son, C. Pac, S. O. Kang, *Inorg. Chem.* **2017**, *56*, 5305–5315; j) J.-L. Liao, P. Rajakannu, P. Gnanasekaran, S.-R. Tsai, C.-H. Lin, S.-H. Liu, C.-H. Chang, G.-H. Lee, P.-T. Chou, Z.-N. Chen, Y. Chi, *Adv. Opt. Mater.* **2018**, *6*, 1800083.

EurJIC
European Journal of Inorganic Chemistry

Minireviews
doi.org/10.1002/ejic.202100663

Chemistry
Europe
European Chemical
Societies Publishing

[13] a) A. Kapturkiewicz, *Anal. Bioanal. Chem.* **2016**, *408*, 7013–7033; b) Y. Chi, T.-K. Chang, P. Ganesan, P. Rajakannu, *Coord. Chem. Rev.* **2017**, *346*, 91–100.

[14] a) E. Baranoff, B. F. E. Curchod, J. Frey, R. Scopelliti, F. Kessler, I. Tavernelli, U. Rothlisberger, M. Grätzel, M. K. Nazeeruddin, *Inorg. Chem.* **2012**, *51*, 215–224; b) Y. Cudré, F. Franco de Carvalho, G. R. Burgess, L. Male, S. J. A. Pope, I. Tavernelli, E. Baranoff, *Inorg. Chem.* **2017**, *56*, 11565–11576; c) W. Dang, X. Yang, Z. Feng, Y. Sun, D. Zhong, G. Zhou, Z. Wu, W.-Y. Wong, *J. Mater. Chem. C* **2018**, *6*, 9453–9464.

[15] a) Y. Tamura, Y. Hisamatsu, S. Kumar, T. Itoh, K. Sato, R. Kuroda, S. Aoki, *Inorg. Chem.* **2017**, *56*, 812–833; b) Y. Tamura, Y. Hisamatsu, A. Kazama, K. Yoza, K. Sato, R. Kuroda, S. Aoki, *Inorg. Chem.* **2018**, *57*, 4571–4589.

[16] a) R. Davidson, Y.-T. Hsu, C. Bhagani, D. Yufit, A. Beeby, *Organometallics* **2017**, *36*, 2727–2735; b) Y. Hisamatsu, S. Kumar, S. Aoki, *Inorg. Chem.* **2017**, *56*, 886–899; c) Y. Kataokaa, K. Okunoa, N. Yanoa, H. Uedaa, T. Kawamotob, M. Handa, *J. Photochem. Photobiol. A* **2018**, *358*, 345–355; d) R. J. Davidson, Y.-T. Hsu, D. Yufit, A. Beeby, *Organometallics* **2018**, *37*, 2003–2006.

[17] a) J. A. G. Williams, A. J. Wilkinson, V. L. Whittle, *Dalton Trans.* **2008**, 2081–2099; b) C.-Y. Kuei, W.-L. Tsai, B. Chou, *Adv. Mater.* **2016**, *28*, 2795–2800; c) C.-Y. Kuei, S.-H. Liu, P.-T. Chou, G.-H. Lee, Y. Chi, *Dalton Trans.* **2016**, *45*, 15364–15373; d) H.-H. Kuo, Y.-T. Chen, L. R. Devereux, C.-C. Wu, M. A. Fox, C.-Y. Kuei, Y. Chi, G.-H. Lee, *Adv. Mater.* **2017**, *29*, 1702464; e) H.-H. Kuo, Z.-L. Zhu, C.-S. Lee, Y.-K. Chen, S.-H. Liu, P.-T. Chou, A. K.-Y. Jen, Y. Chi, *Adv. Sci.* **2018**, 1800846; f) P. Gnanasekaran, Y. Yuan, C.-S. Lee, X. Zhou, A. K.-Y. Jen, Y. Chi, *Inorg. Chem.* **2019**, *58*, 10944–10954; g) L.-Y. Hsu, Q. Liang, Z. Wang, H.-H. Kuo, W.-S. Tai, S.-J. Su, X. Zhou, Y. Yuan, Y. Chi, *Chem. Eur. J.* **2019**, *25*, 15375–15386; h) L.-Y. Hsu, D.-G. Chen, S.-H. Liu, T.-Y. Chiu, C.-H. Chang, A. K.-Y. Jen, P.-T. Chou, Y. Chi, *ACS Appl. Mater. Interf.* **2020**, *12*, 1084–1093; i) W.-S. Tai, P. Gnanasekaran, Y.-Y. Chen, W.-Y. Hung, X. Zhou, T.-C. Chou, G.-H. Lee, P.-T. Chou, C. You, Y. Chi, *ACS Appl. Mater. Interfaces* **2021**, *13*, 15437–15447.

[18] a) Y.-S. Li, J.-L. Liao, K.-T. Lin, W.-Y. Hung, S.-H. Liu, G.-H. Lee, P.-T. Chou, Y. Chi, *Inorg. Chem.* **2017**, *56*, 10054–10060; b) Y. Yuan, P. Gnanasekaran, Y.-W. Chen, G.-H. Lee, S.-F. Ni, C.-S. Lee, Y. Chi, *Inorg. Chem.* **2020**, *59*, 523–532.

[19] J.-P. Sauvage, J.-P. Collin, J.-C. Chambron, S. Guillerez, C. Coudret, V. Balzani, F. Barigelletti, L. De Cola, L. Flamigni, *Chem. Rev.* **1994**, *94*, 993–1019.

[20] E. Baranoff, J.-P. Collin, L. Flamigni, J.-P. Sauvage, *Chem. Soc. Rev.* **2004**, *33*, 147–155.

[21] a) D. A. K. Vezzu, J. C. Deaton, J. S. Jones, L. Bartolotti, C. F. Harris, A. P. Marchetti, M. Kondakova, R. D. Pike, S. Huo, *Inorg. Chem.* **2010**, *49*, 5107–5119; b) S. Huo, C. F. Harris, D. A. K. Vezzu, J. P. Gagnier, M. E. Smith, R. D. Pike, Y. Li, *Polyhedron* **2013**, *52*, 1030–1040; c) T. B. Fleetham, L. Huang, K. Klimes, J. Brooks, J. Li, *Chem. Mater.* **2016**, *28*, 3276–3282; d) X. Wang, T. Peng, C. Nguyen, Z.-H. Lu, N. Wang, W. Wu, Q. Li, S. Wang, *Adv. Funct. Mater.* **2017**, *27*, 1604318; e) C.-H. Lee, M.-C. Tang, F. K.-W. Kong, W.-L. Cheung, M. Ng, M.-Y. Chan, V. W.-W. Yam, *J. Am. Chem. Soc.* **2020**, *142*, 520–529; f) G. Li, F. Zhan, J. Zheng, Y.-F. Yang, Q. Wang, Q. Chen, G. Shen, Y. She, *Inorg. Chem.* **2020**, *59*, 3718–3729.

[22] a) P. K. Chow, C. Ma, W.-P. To, G. S. M. Tong, S.-L. Lai, S. C. F. Kui, W.-M. Kwok, C.-M. Che, *Angew. Chem. Int. Ed.* **2013**, *52*, 11775–11779; *Angew. Chem.* **2013**, *125*, 11991–11995; b) Z.-Q. Zhu, T. Fleetham, E. Turner, J. Li, *Adv. Mater.* **2015**, *27*, 2533–2537; c) P.-K. Chow, G. Cheng, G. S. M. Tong, C. Ma, W.-M. Kwok, W.-H. Ang, C.-Y.-S. Chung, C. Yang, F. Wang, C.-M. Che, *Chem. Sci.* **2016**, *7*, 6083–6098; d) Z.-Q. Zhu, C.-D. Park, K. Klimes, J. Li, *Adv. Opt. Mater.* **2019**, *7*, 1801518; e) G. Li, Ji. Zheng, X. Fang, K. Xu, Y.-F. Yang, J. Wu, L. Cao, J. Li, Y. She, *Organometallics* **2021**, *40*, 472–481.

[23] J.-Y. Tsai, C. Xia, M. A. Esteruelas, *Osmium(IV) Complexes for OLED Material.*, U.S. Patent Appl. 14/075653, filled 8 november 2013, US20140138653A1 (**2014**), Patent No. US10069090B2 (**2018**).

[24] M. A. Esteruelas, A. M. López, M. Oliván, *Chem. Rev.* **2016**, *116*, 8770–8847.

[25] O. Crespo, B. Eguillor, M. A. Esteruelas, I. Fernández, J. García-Raboso, M. Gómez-Gallego, M. Martín-Ortiz, M. Oliván, M. A. Sierra, *Chem. Commun.* **2012**, *48*, 5328–5330.

[26] B. Eguillor, M. A. Esteruelas, I. Fernández, M. Gómez-Gallego, A. Lledós, M. Martín-Ortiz, Montserrat Oliván, E. Oñate, M. A. Sierra, *Organometallics* **2015**, *34*, 1898–1910.

[27] L. Cancela, M. A. Esteruelas, A. M. López, M. Oliván, E. Oñate, A. San-Torcuato, A Vélez, *Organometallics* **2020**, *39*, 2102–2115.

[28] L. Cancela, M. A. Esteruelas, J. Galbán, M. Oliván, E. Oñate, A. Vélez, J. C. Vidal, *Inorg. Chem.* **2021**, *60*, 2783–2796.

[29] a) M. B. Robin, P. Day, *Adv. Inorg. Chem. Radiochem.* **1968**, *10*, 247–422; b) M. Parthey, M. Kaupp, *Chem. Soc. Rev.* **2014**, *43*, 5067–5088.

[30] a) B. S. Brunschwig, C. Creutz, N. Sutin, *Chem. Soc. Rev.* **2002**, *31*, 168–184; b) P. Aguirre-Etcheverry, D. O'Hare, *Chem. Rev.* **2010**, *110*, 4839–4864.

[31] R. G. Alabau, M. A. Esteruelas, M. Oliván, E. Oñate, *Organometallics* **2017**, *36*, 1848–1859.

[32] C. Xia, J.-Y. Tsai, M. A. Esteruelas; R. Gómez, M. Oliván, E. Oñate, *Organic electroluminescent materials and devices*, U.S. Patent Appl. 14/996448, filled 15 January 2016, US20160240799A1 (**2016**), Patent No. US9929361B2 (**2018**).

[33] B. Eguillor, M. A. Esteruelas, V. Lezáun, M. Oliván, E. Oñate, *Chem. Eur. J.* **2017**, *23*, 1526–1530.

[34] R. Castro-Rodrigo, M. A. Esteruelas, D. Gómez-Bautista, V. Lezáun, A. M. López, M. Oliván, E. Oñate, *Organometallics* **2019**, *38*, 3707–3718.

[35] L. Casarrubios, M. A. Esteruelas, C. Larramona, J. G. Muntaner, E. Oñate, M. A. Sierra, *Inorg. Chem.* **2015**, *54*, 10998–11006.

[36] R. G. Alabau, B. Eguillor, J. Esler, M. A. Esteruelas, M. Oliván, E. Oñate, J.-Y. Tsai, C. Xia, *Organometallics* **2014**, *33*, 5582–5596.

[37] a) K. S. Yook, J.-Y. Lee, *Adv. Mater.* **2012**, *24*, 3169–3190; b) J. B. Kim, S. H. Han, K. Yang, S. K. Kwon, J. J. Kim, Y. H. Kim, *Chem. Commun.* **2015**, *51*, 58–61; c) Y.-J. Cho, S.-Y. Kim, J.-H. Kim, J. Lee, D. W. Cho, S. Yi, H.-J. Son, W.-S. Han, S. O. Kang, *J. Mater. Chem. C* **2017**, *5*, 1651–1659; d) Z. Chen, L. Wang, S. Su, X. Zheng, N. Zhu, C.-L. Ho, S. Chen, W.-Y. Wong, *ACS Appl. Mater. Interfaces* **2017**, *9*, 40497–40502; e) L. Zhang, Z.-P. Yan, Y.-X. Zheng, *Dalton Trans.* **2019**, *48*, 9744–9750.

[38] R. G. Alabau, M. A. Esteruelas, M. Oliván, E. Oñate, A. U. Palacios, J.-Y. Tsai, C. Xia, *Organometallics* **2016**, *35*, 3981–3995.

[39] M. A. Esteruelas, E. Oñate, A. Palacios, J.-Y. Tsai, C. Xia, *Organometallics* **2016**, *35*, 2532–2542.

[40] M. A. Esteruelas, E. Oñate, A. U. Palacios, *Organometallics* **2017**, *36*, 1743–1755.

[41] P.-L. T. Boudreault, M. A. Esteruelas, A. M. López, E. Oñate, E. Raga, J.-Y. Tsai, *Inorg. Chem.* **2020**, *59*, 15877–15887.

[42] A. J. Edwards, S. Elipe, M. A. Esteruelas, F. J. Lahoz, L. A. Oro, C. Valero, *Organometallics* **1997**, *16*, 3828–3836.

[43] M. L. Buil, S. Elipe, M. A. Esteruelas, E. Oñate, E. Peinado, N. Ruiz, *Organometallics* **1997**, *16*, 5748–5755.

[44] P.-L. T. Boudreault, M. A. Esteruelas, E. Mora, E. Oñate, J.-Y. Tsai, *Organometallics* **2019**, *38*, 2883–2887.

[45] P.-L. T. Boudreault, M. A. Esteruelas, E. Mora, E. Oñate, J.-Y. Tsai, *Organometallics* **2018**, *37*, 3770–3779.

[46] V. Adamovich, S. Bajo, P.-L. T. Boudreault, M. A. Esteruelas, A. M. López, J. Martín, M. Oliván, E. Oñate, A. U. Palacios, A. San-Torcuato, J.-Y. Tsai, C. Xia, *Inorg. Chem.* **2018**, *57*, 10744–10760.

[47] J. A. G. Williams, *Chem. Soc. Rev.* **2009**, *38*, 1783–1801.

[48] A. J. Wilkinson, A. E. Goeta, C. E. Foster, J. A. G. Williams, *Inorg. Chem.* **2004**, *43*, 6513–6515.

[49] A. J. Wilkinson, H. Puschmann, J. A. K. Howard, C. E. Foster, J. A. G. Williams, *Inorg. Chem.* **2006**, *45*, 8685–8699.

[50] P.-L. T. Boudreault, M. A. Esteruelas, D. Gómez-Bautista, S. Izquierdo, A. M. López, E. Oñate, E. Raga, J.-Y. Tsai, *Inorg. Chem.* **2020**, *59*, 3838–3849.

[51] B. Soro, S. Stoccoro, G. Minghetti, A. Zucca, M. A. Cinellu, S. Gladiali, M. Manassero, M. Sansoni, *Organometallics* **2005**, *24*, 53–61.

[52] M. A. Esteruelas, D. Gómez-Bautista, A. M. López, E. Oñate, J.-Y. Tsai, C. Xia, *Chem. Eur. J.* **2017**, *23*, 15729–15737.

[53] a) J. Li, A. C. Grimsdale, *Chem. Soc. Rev.* **2010**, *39*, 2399–2410; b) Y. Tao, Q. Wang, C. Yang, C. Zhong, K. Zhang, J. Qin, D. Ma, *Adv. Funct. Mater.* **2010**, *20*, 304–311; c) M. A. Reddy, A. Thomas, G. Mallesham, B. Sridhar, V. J. Rao, K. Bhanuprakash, *Tetrahedron Lett.* **2011**, *52*, 6942–6947; d) M. S. Park, J.-Y. Lee, *Org. Electron.* **2013**, *14*, 1291–1296; e) G. H. Kim, R. Lampande, M. J. Park, H. W. Bae, J. H. Kong, J. H. Kwon, J. H. Park, Y. W. Park, C. E. Song, *J. Phys. Chem. C* **2014**, *118*, 28757–28763; f) H. Shi, D. Xin, S.-D. Bai, L. Fang, X.-E. Duan, J. Roose, H. Peng, S. Chen, B. Z. Tang, *Org. Electron.* **2016**, *33*, 78–87; g) M. Reig, G. Bubniene, W. Cambarau, V. Jankauskas, V. Getautis, E. Palomares, E. Martínez-Ferrero, D. Velasco, *RSC Adv.* **2016**, *6*, 9247–9253.

[54] C. Moreno-Cabrerizo, A. Ortega-Martínez, M. A. Esteruelas, A. M. López, C. Nájera, J. M. Sansano, *Eur. J. Org. Chem.* **2020**, 3101–3109.

[55] V. Adamovich, P.-L. T. Boudreault, M. A. Esteruelas, D. Gómez-Bautista, A. M. López, E. Oñate, J.-Y. Tsai, *Organometallics* **2019**, *38*, 2738–2747.

[56] M. A. Esteruelas, A. M. López, E. Oñate, A. San-Torcuato, J.-Y. Tsai, C. Xia, *Inorg. Chem.* **2018**, *57*, 3720–3730.

[57] M. A. Esteruelas, A. M. López, E. Oñate, A. San-Torcuato, J.-Y. Tsai, C. Xia, *Organometallics* **2017**, *36*, 699–707.

[58] a) C.-H. Chien, S. Fujita, S. Yamoto, T. Hara, T. Yamagata, M. Watanabe, K. Mashima, *Dalton Trans.* **2008**, 916–923; b) H. Tsurugi, S. Fujita, G. Choi, T. Yamagata, S. Ito, H. Miyasaka, K. Mashima, *Organometallics* **2010**, *29*, 4120–4129.

[59] L. Benavent, P.-L. T. Boudreault, M. A. Esteruelas, A. M. López, E. Oñate, J.-Y. Tsai, *Inorg. Chem.* **2020**, *59*, 12286–12294.

[60] Y.-S. Li, J.-L. Liao, K.-T. Lin, W.-Y. Hung, S.-H. Liu, G.-H. Lee, P.-T. Chou, Y. Chi, *Inorg. Chem.* **2017**, *56*, 10054–10060.

[61] Y. Yuan, P. Gnanasekaran, Y.-W. Chen, G.-H. Lee, S.-F. Ni, C.-S. Lee, Y. Chi, *Inorg. Chem.* **2020**, *59*, 523–532.

[62] A. Adamovich, L. Benavent, P.-L. T. Boudreault, M. A. Esteruelas, A. M. López, E. Oñate, J.-Y. Tsai, *Inorg. Chem.* **2021**, *60*, 15, 11347–11363.